Mesopithecus pentelicus from the Turolian locality of Kryopigi (Kassandra, Chalkidiki, Greece)

Georgios Lazaridis[a], Evangelia Tsoukala[a], Todd C. Rae[b], Asier Gómez-Olivencia[c,d,e,f], Doris Nagel[g], Antonis Bartsiokas[h]

[a] School of Geology, Aristotle University (AUTH), 54124 Thessaloniki, Greece
[b] Centre for Research in Evolutionary, Social & InterDisciplinary Anthropology, University of Roehampton, Holybourne Avenue, London SW15 4JD, United Kingdom
[c] Departamento de Estratigrafía y Paleontología, Facultad de Ciencia y Tecnología, Euskal Herriko Unibertsitatea (UPV/EHU). Barrio Sarriena s/n, 48940 Leioa, Spain
[d] IKERBASQUE, Basque Foundation for Science, Spain
[e] Équipe de Paléontologie Humaine, UMR 7194, CNRS, Département de Préhistoire, Muséum National d'Histoire naturelle, Musée de l'Homme, 17, Place du Trocadéro, 75016 Paris, France
[f] Centro UCM-ISCIII de Investigación sobre Evolución y Comportamiento Humanos, Avda. Monforte de Lemos 5 (Pabellón 14), 28029 Madrid, Spain
[g] Department of Palaeontology, University of Vienna, Althanstrasse 14, 1090 Vienna, Austria
[h] Laboratory of Anthropology, Department of History and Ethnology, Democritus University of Thrace, P. Tsaldari 1, 69100, Komotini, Greece

Key-words: Primates; Cercopithecidae; *Mesopithecus pentelicus*; Late Miocene; Turolian; Kryopigi

Corresponding author:
Georgios Lazaridis
School of Geology, Aristotle University (AUTH), 54124 Thessaloniki, Greece.
geolaz@geo.auth.gr

Abstract

New material of the Mio-Pliocene colobine *Mesopithecus* from the Turolian locality of Kryopigi (Greece) is described here. It includes a complete skull with the atlas attached and other dental and postcranial elements representing at least five individuals (four males and one female). The material is compared with *M. delsoni*, *M. pentelicus*, *M. monspessulanus* and intermediate forms from more than a dozen Turolian localities of the Greco-Iranian province. These comparisons support the attribution of the Kryopigi material to *M. pentelicus*. The chronostratigraphic distribution of *Mesopithecus* species and intermediate forms suggests that the Kryopigi fauna could be dated as younger than the Perivolaki locality with *M. delsoni/pentelicus* (7.1-7.3 Ma, MN12) and older than the Dytiko localities with *M.* aff. *pentelicus*, *M.* cf. *pentelicus* and *M.* cf. *monspessulanus* (?middle MN13). The dimensions of the atlas are within the distribution of extant colobines. The skull shows bite-marks, probably caused by the hyaena *Adcrocuta eximia*.

1. **Introduction**

Mesopithecus is a well-known colobine primate recovered from several Late Miocene and Pliocene localities in the Balkan states (Fig. 1) including Greece (Pikermi, Chomateri, Perivolaki, Nikiti, Ravin des Zouaves-5, Vathylakkos-2,3, Ravin X, Dytiko localities and Maramena), Bulgaria (Kalimantsi, Gorna Sushitsa, Kromidovo, Hadjidimovo), and the Former Yugoslavian Republic of Macedonia (Titov Veles). It is also present in Hungary, Ukraine, Italy, Germany, France, the United Kingdom, Romania, and the Iberian Peninsula (e.g., Andrews et al., 1996; Rook, 1999; Koufos et al., 2003; Delson et al., 2005; Koufos, 2008, 2009a, b; Alba et al., 2013, 2014, 2015; Marigó et al., 2014). It is absent from Asia Minor, although it appears again in the Turolian localities in Afghanistan (Molayan), Iran (Maragheh), Pakistan (Siwaliks: Harrison and Delson, 2007) and China (Jablonski et al., 2011; Ji et al., 2013). There are four species of the genus *Mesopithecus* currently recognized: *Mesopithecus pentelicus* (Wagner, 1839) (middle Turolian, type locality Pikermi), *Mesopithecus monspessulanus* (Gervais, 1849) (Ruscinian, type locality Montpelier), *Mesopithecus sivalensis* (Lydekker, 1878) (late Miocene, type locality Middle Siwaliks; Harrison and Delson, 2007) and *Mesopithecus delsoni* (Bonis et al., 1990) (Early Turolian, type locality Ravin des Zouaves-5, Axios valley), although there is some disagreement on the validity of the last species (Zapfe, 1991; Delson, 1994; Andrews et al., 1996; Delson et al., 2000). Here, we provide a detailed report on new *Mesopithecus* material from the Turolian locality of Kryopigi in Greece (Tsoukala and Bartsiokas, 2008).

INSERT FIGURE 1 AROUND HERE

1.1. Locality

Kryopigi village is located about 100 km south-southeast of Thessaloniki (N 40˚ 02′ 4.05′′, E 023˚ 28′ 19.304′′, in the Kassandra (Pallene, Phlegra) peninsula of Chalkidiki, Macedonia, Greece (Fig. 1). The Kryopigi fossiliferous layer belongs to the Triglia Formation, according to the stratigraphic division of Syrides (1990), and consists of fluvial sediments of approximately three meters in thickness. The majority of the specimens were collected from a horizon of about two meters in thickness. The Kryopigi fauna is diverse and comprises 32 vertebrate taxa (including mammals, birds and reptiles), excavated systematically over the last 15 years by a team from the Thessaloniki Aristotle University (scientific supervision led by E.T.). In 2010 and 2012, a second team from the University of Vienna (headed by D.N.) joined the excavation. The collection consists of more than 7,000 specimens. Kryopigi consists of a single locality and horizon and is thus more restricted spatially and temporally than other *Mesopithecus*-bearing localities where the collections include material from various excavation sites (e.g., Pikermi, Kalimantsi). The faunal list of the locality is given in Table 1. The age of the fauna is dated to the second half of the Turolian, in late MN12 or early MN13 biozones, between 7.3-6.4 Ma (Lazaridis, 2015).

The paleoecology and taphonomy of the locality indicate that the bones were accumulated due to carnivore activity during repeated dry periods (Lazaridis, 2015). The material was buried quickly and shows no signs of transport. The environment and landscape of Kryopigi appears to have been open and savanna-like, with a hot and dry climate and mean annual temperature of at least 15^{o}C (Lazaridis, 2015). However, there are some fauna that show adaptation to a more closed and forested environment.

Primate material from Kryopigi was first described by Tsoukala and Bartsiokas (2008), who attributed a maxilla to *M. pentelicus*, and an isolated M^3 to *Mesopithecus* sp. due to its slightly larger size than that of *M. pentelicus* from the type locality Pikermi. In addition to that material, the authors illustrated and briefly discussed a very well-preserved skull with the atlas attached to the foramen magnum. We describe that specimen in detail here, along with various other dental and postcranial elements corresponding to the primate material found at Kryopigi.

INSERT TABLE 1 AROUND HERE

1.2. Institutional Abbreviations

LGPUT=Laboratory of Geology and Paleontology, University of Thessaloniki; MNHN=Muséum national d'Histoire naturelle (Paris); RMCA=Royal Museum for Central Africa (Tervuren, Belgium); NHM=Natural History Museum (London).

2. Materials and methods

All specimens are housed in the Museum of Paleontology at the Laboratory of Geology and Paleontology, University of Thessaloniki (LGPUT) with the locality acronym KRY (Kryopigi).

Linear measurements were taken on the cranium, mandible, dentition and postcranial material using a digital caliper (accuracy ± 0.01 mm). All measurements are given in millimeters. Bivariate and multivariate analysis and statistical tests were performed using PAST 2.17 (Hammer et al., 2001). The level of statistical significance was set at $\alpha = 0.05$. Dental dimensions were size-adjusted using the geometric mean (GM) of all variables. Principal component analysis (PCA) of the teeth was carried out using these size-adjusted variables. Molar and premolar dimensions were used in the multivariate analysis; excluding premolar length, due to significant intraspecific variation seen in the high values of the coefficients of variation (CV). For example, P_3 length of *M. pentelicus* shows a CV of 12.2 for males and 12.1 for females (Zapfe, 1991) and P_4 length of *M. delsoni* males from the type locality (CV= 21.6; Bonis et al., 1990) display much higher CVs than the rest of the measurements. In the published material, incisors and canines are commonly absent; therefore, they were excluded from the analysis to reduce ambiguity due to missing data.

To assess the overall configuration of the cranium, geometric morphometric (GM) analysis was performed. Serial coronal CT scans (512×512) of the skull (KRY5600) were obtained (in collaboration with Prof. A. Dimitriadis, Aristotle University of Thessaloniki) using a Siemens Somatom Plus 4 scanner (140kV, 129mA) at 1mm slice intervals with a pixel size of 0.292. Three-dimensional virtual crania were derived from these data. These were compared with scans obtained from other extant and extinct cercopithecoid genera (Rae, 2008), using Avizo 7.1 (FEI Visualization Sciences Group, Mérignac Cedex, France). One 3D virtual cranium for each genus (except *Mesopithecus*, for which a second cranium from Pikermi was included; M.8947, Natural History Museum, London) was created from the CT data using Avizo 7.1 (FEI Visualization Sciences Group, Mérignac Cedex, France). The nine standard Type 1 landmarks used were selected because they are preserved in an undistorted position from the left side of KRY5600. Landmarks used for geometric morphometric comparisons were: 1. Glabella; 2. Alare; 3. Nasospinale; 4. Prosthion; 5. Ectomolare; 6. Zygomaxillare anterior; 7. Orbitale; 8. Frontomalare orbitale; 9. Frontotemporale. For the Pikermi *Mesopithecus* M.8947, a mirror image of the right side was used, and the position of frontomalare orbitale was estimated, due to taphonomic displacement. Landmark coordinates were recorded using Avizo 8 (Visualization Sciences Group, Burlington, MA). Landmark data were analyzed using MorphoJ (Klingenberg, 2011). After a standard Procrustes fit, the resulting data were subjected to a principal component analysis to assess the morphological affinities of the Kryopigi material compared to extant colobine and cercopithecine taxa.

3. Systematic paleontology

Order: Primates Linneaus, 1758

Semiorder: Haplorhini Pocock 1918

Suborder: Anthropoidea Mivart, 1864

Infraorder: Catarrhini Geoffroy Saint-Hilaire, 1812

Superfamily: Cercopithecoidea Gray, 1821

Family: Cercopithecidae Gray, 1821

Subfamily: Colobinae Blyth, 1863

Genus: *Mesopithecus* Wagner, 1839

Mesopithecus pentelicus Wagner, 1839

3.1. Material and descriptions

The *Mesopithecus* fossils from Kryopigi are listed in Table 2 and shown in Figures 2-5.

INSERT TABLE 2 AND FIGURES 2 TO 5 AROUND HERE

3.2. Skull

The skull (KRY5600) is almost complete. Only the left I^2, right occipital condyle and a part of the right orbit are missing (Fig. 2; Table 3). As is commonly the case for *Mesopithecus* remains, it shows some very limited and weak deformation. The facial part of the cranium is in a very good state of preservation. The zygomatic arches are completely preserved and stout although they have lost their symmetry. They are compressed from the right towards to the left side of the skull. This deformation also affects the whole posterior neurocranium.

The facial angle is short and upright (~ 52°). The quadrangular orbits are separated by a relatively narrow interorbital region (for a colobine) and accompanied by thick and continuous supraorbital tori, as in other male individuals of *Mesopithecus*. A slight depression is present behind them. The temporal lines extend from the orbits back to the parietal-occipital suture. They are strongly developed in the first third of their length and weaker in the posterior two thirds. The temporal lines do not meet posterior to bregma. The orbits are about 25 mm deep. There are four infraorbital foramina arranged parallel to a line connecting the uppermost border of nasals and the processus zygomaticus maxillae. The latter is strongly protruding and better preserved on the left side. The roots of the zygomatic arches are above the junction between M^1-M^2. The nasal fossa is long and narrow. The anterior part is pointed, and the posterior end is placed above P^3. The nasal bones are triangular in shape and extend upwards to approximately two thirds the height of the interorbital region. The palate is slightly deformed (compressed on the left side). The postcanine tooth rows are curved, so that the lateral borders of the palate are convex. The choanae are deep, more or less ovoid in shape and extend to the posterior half of M^3. The foramen palatinum majus is placed at the level of the junction between M^2-M^3. The fossae glenoidea for the articulation of the mandible condyles are both displaced posteriorly of their original position, as indicated by the mandible when it is in its anatomical position. The right side is the best preserved. Standard linear measurements of the cranium are given in Table 3.

INSERT FIGURE 2 & TABLE 3 AROUND HERE

Three large holes appear in the left parietal of the KRY5600 skull (Fig. 2C, D). They are probably the consequence of compression, as suggested by the radial bone fracture and the presence of broken bone in the bottom of each hole. These defects resemble puncture marks commonly attributed to carnivore bites. The first (and larger) bite mark is located in the frontal, in the area of postorbital constriction; the second and third marks are at distances of 19 mm and 23 mm posteriorly of the first, respectively. The latter two are ~6 mm in diameter and may correspond to large carnivore premolars, whereas the larger one probably corresponds to a canine. On the right side, there are two more presumed bite marks, 8 mm in diameter and 8 mm distance from each other, just above the external auditory meatus.

3.3. Mandible

The mandible is almost complete and well-preserved except for the right corpus, which appears to be crushed and deformed towards the left side. The mandibular corpus is relatively shallow for a colobine. In lateral view, the anterior face of the symphysis forms an angle of 120° with the inferior border of the corpus. The symphyseal foramen is placed below the anterior roots of P_4, near the midpoint of the corpus height. The symphysis has a convex anterior face and lacks constriction. The inferior transverse torus is rather weak. The fossa genioglossa is weakly developed. The alveolar plane is strongly inclined backwards (Fig. 3). Standard linear measurements of the mandible are given in Table 4.

INSERT FIGURE 3 & TABLE 4 AROUND HERE

3.4. Upper dentition

The first upper incisor is longer mesiodistally than the second. The upper canine is stout and tall (12.8 mm in the skull KRY5600), with a subtriangular cross-section and a well expressed mesial groove, indicating a male individual. This is the case for all of the other canines in the Kryopigi sample, as well. The premolars display a tall paracone and a short protocone (Fig. 2G). In both premolars, the anterior fovea is smaller than the posterior one. The molars are bilophodont. M^3 possesses a small distal lobe that is positioned slightly lingually, and with a distoconule that is characterized by a well-developed mesial lingual cleft (in KRY5600). Although there are no posterior accessory cuspules, there is a well-developed metaconule in the distal fovea of the isolated second molar KRY1000, which also shows a strong mesial buccal cleft. In KRY1000, the ratios of posterior to anterior width and length of posterior to anterior lobe are intermediate to those characteristic of M^2 and M^3. However, its square shape, due to the flat distal facet, the absence of a distoconule (present in M^3), and the constriction between the two lobes all support its attribution to M^2. M^3 possesses a smaller distal lobe that is slightly shifted lingually and has a distoconule that is characterized by a well-developed mesial lingual cleft (in KRY5600).

3.5. Lower dentition

The first and second lower incisors are almost equally long mesiodistally and the incisor row is arch-shaped. The canines are relatively stout and sub-triangular in cross-section. There is a honing facet on P_3, with a strong protoconid and weak metaconid. The protoconid and metaconid of P_4 are almost equal in size, but the latter is slightly higher. Moreover, there is a large distal fovea. In the molars, the lingual cuspids (metaconid, entoconid) are higher than those in the buccal side (hypoconid, protoconid). They do not display any accessory cuspids. The talonid of M_3 is small and lacks a distal groove. It is shifted buccally, resulting in asymmetry in respect to the long axis of the tooth (Fig. 3G). The standard linear measurements of the dentition are given in Table 5.

INSERT TABLE 5 AROUND HERE

3.6. Atlas

The first cervical vertebra consists of the anterior arch, the right lateral mass, the right transverse process (although partially broken), a fragment of the posterior arch from the right side and a fragment of the left lateral mass. The upper articular facet is complete, but not so the lower one (Fig. 4). This specimen is the result of a reconstruction from six different fragments. There is a small amount of distortion between the fragments that compose the lateral mass and the anterior arc, but this does not affect the measurements reported here.

From the upper articular facet it displays two bony arches: one that goes to the transverse process and the other to the posterior arch, encircling the passage of the vertebral artery. These arches are often present in colobines and other cercopithecids although the frequency varies. In fact, we have noted that in extant species the transverse process morphology is highly variable in colobines. KRY 5600, although not completely preserved, fits within the range of variation of the extant taxa.

INSERT FIGURE 4 AROUND HERE

3.7 Limb bones

The postcranium of *Mesopithecus* was fully described in detail by Zapfe (1991) and here only important points are discussed. The left distal humerus KRY5620 (Table 6; Fig. 5A) belongs to a male, and probably to the same individual as the left proximal ulna KRY5621 (see below), as the two were found in close proximity and are similar in size and preservation. A little more than a quarter of the total length of the humerus is preserved in very good condition. All morphological features are well defined. The relatively short, deep, and high trochlea displays a well-defined and distally protruding medial rim, and it is separated from the capitulum by a relatively weak keel and wide neck (Fig. 5 A1). The capitulum is medially high, and the fossa olecrani (without foramen supratrochleare) is high and deep (6.8 mm deep). This fossa is wider than high (Fig. 5 A2), which is characteristic of a male individual (Zapfe, 1991). The epicondylus lateralis is low but present, and a significant large, crest-like margo lateralis originates from it (Fig. 5 A3). The fossa coronoidea is well separated from, and wider than, the fossa radialis. In posterior aspect the epicondylus medialis, above the sulcus ulnaris (Fig. 5 A4), is projected posteriorly.

INSERT TABLE 6 AROUND HERE

The left proximal ulna KRY5621 (Table 7; Fig. 5B) probably belongs to the same male as KRY5620 (see above). A little more than a quarter of the total length of the ulna is preserved in good condition. The proximal part of the diaphysis is almost straight. The olecranon is relatively long and moderately retroflected. The oblique and relatively wide incisura semilunaris extends medially from the beak and ends in the processus coronoideus, the pointed tip of which is missing. The deeply hollowed incisura radialis is single, and drop-shaped.

INSERT TABLE 7 AROUND HERE

The left distal radius KRY1309 (Table 8; Fig. 5C) also belongs to a male. A little less than a quarter of the total length of the radius is preserved in moderately good condition. The furrow for the musculi extensorum carpi radialium is well-developed due to the pronounced margo dorsalis (Fig. 5 C1). The processus styloideus is obtuse but clearly protrudes (Fig. 5 B2), followed by an oval to sub-triangular hollow facies articularis carpea. The incisura ulnaris is clear and distinct (Fig. 5 C3).

INSERT TABLE 8 AROUND HERE

The right astragalus KRY8900 (Fig. 5D) is more robust than the left (KRY2772, Fig. 5E) and other right (KRY2773, Fig. 5F) astragali. This suggests that the former is probably male, while the latter two belonged to female individuals (Table 9). The trochlea tali is distally wide and asymmetrical, tapering posteriorly. The medial tubercle is more developed, swollen and protruding in the male talus than in the female. The collum tali is robust and the facies articularis navicularis is wide and more developed in the male than in the female tali, followed by a more rectangular facies articularis calcanearis media and deeper sulcus tali in the former. There is a distinct, rounded fovea just above the comma-shaped and hollow facies malleolaris medialis in the male, whereas it is less distinct on the female tali. There is a deep, elongated groove between the facies malleolaris lateralis and the considerably concave facies articularis calcanearis posterior (Fig. 5 D2-F2).

INSERT TABLE 9 AROUND HERE

The left and right calcanei (Table 10), KRY2771 (Fig. 5G) and KRY2770 (Fig. 5H), respectively, probably belong to females based on size and compared to specimens from Pikermi (Table 10), the latter being better preserved than the former. On the antero-lateral side of the corpus, just below the poorly-fused tuber calcanei, there is a marked, oval-shaped groove. The sustentaculum tali protrudes with oval-shaped and slightly hollowed facies articularis talaris media, below which a crest-like edge extends up to the medial end of the facies articularis cuboidea.

INSERT TABLE 10 AROUND HERE

There are four metapodial fragments: two proximal (Fig. 5I-J) and two distal (Fig. 5K-L). The distal trochlea bears a slight median crest on the posterior side, whereas the condyles are well marked (Fig. 5 K2-L2) (Table 11).

The four proximal fragments of phalanges (Ph1) (Fig. 5M-P) show broad articular surfaces for the metapodial trochlea and left and right eminences posteriorly, probably for the lateral sesamoids (Fig. 5 M2-O2) (Table 12).

INSERT FIGURE 5 & TABLES 11-12 AROUND HERE

4. Comparisons

The Kryopigi *Mesopithecus* material is compared here with that from other Balkan localities such as Pikermi, Ravin des Zouaves, Vathylakkos, Perivolaki, Dytiko, Maramena in Greece, Hadjidimovo, Kalimantsi, Gorna Sushitsa, Kromidovo in Bulgaria, Maraghah in Iran and Molayan in Afganistan. Overall, the skull displays the diagnostic features of *Mesopithecus* (Delson, 1973): an upright face, moderately enlarged mandibular angle, relatively constant mandibular corpus height between M_3 and P_4 and high, narrow choanae. The dentition also matches that of known *Mesopithecus*, with sub-rectangular and high crowned, asymmetrical, quadricuspid, molariform teeth that are straight sided with asymmetrical distal margins in the upper jaw, and that have deep medial lingual notches and reduced trigonid basins in the lower jaw (Delson, 1973).

4.1. Skull

As the majority of *Mesopithecus* cranial material is crushed and/or deformed, it is difficult to compare with other remains. Furthermore, some important *Mesopithecus* localities, such as Ravin des Zouaves-5 (type locality of *M. delsoni*) in Axios, lack cranial material. However, PCA of interorbital width, supraorbital thickness, nasion-prosthion distance, maximum palatal breadth and maximum nasal aperture width was performed using data gathered from Kryopigi RY5600, and raw data for *M. pentelicus* from Pikermi published by Delson (1973) and Zapfe, (1991). Material of the same species from Kalimantsi (Koufos et al., 2003), and of *M.* aff. *delsoni* from Hadjidimovo (Koufos et al., 2003) was also included. The horizontal axis (PC1) of the scatter plot (Fig. 6) is positively influenced by all variables (see histogram of loadings in the lower left corner of the diagram and biplot), but mostly by nasion-prosthion distance. Smaller specimens plot to the left, as is the case for the Pikermi females. Nasion-prosthion distance has a negative loading on PC2, which is dominated by the breadth of palate and nasal aperture. Those specimens with the narrower palates/nasal apertures plot lower down the axis. Relative to the previously known specimens included in the analysis, KRY5600 shows a narrow palate (due to compressed left part) and nasal aperture. It falls inside the 95% confidence ellipses for both male and female *M. pentelicus*. The only specimens outside these ellipses are a skull from Vathylakkos-2 referred to *M. pentelicus/delsoni* (e.g., Koufos, 2009a) and a female skull of *M.* aff. *delsoni* from Hadjidimovo (Koufos et al., 2003).

INSERT FIGURE 6 AROUND HERE

In the GM analysis of the skull, PC1 accounts for ~60% of the variance and is significantly associated with centroid size; as such, it probably represents an allometric size component and is not illustrated here. Larger taxa with increased prognathism are negatively loaded on PC1. PC2 and PC3 (7.554% and 7.324% of the total variance, respectively) are plotted against each other in Figure 7. PC3 shows moderate separation of the colobines (top) from the cercopithecines (bottom), albeit with some overlap. The stem cercopithecoid *Victoriapithecus* (KNM-MB 29100; Rae et al., 2002) is a clear outlier on this axis. KRY5600 falls near the *M. pentelicus* specimen from Pikermi (M.8947) analyzed here, supporting the allocation of the new material to this taxon; both are situated near the odd-nosed colobines *Nasalis*, *Simias* and *Rhinopithecus* in morphospace.

INSERT FIGURE 7 AROUND HERE

4.2. Upper dentition

Five M^2s (Fig. 8A) and two M^3s (Fig. 8B) from Kryopigi are compared on bivariate scatter diagrams of length versus breadth. M^2 is the only tooth represented by more than two specimens. In both bivariate comparisons, the material from Kryopigi overlaps with the area occupied by male individuals of *M. pentelicus* from Pikermi; thus, the isolated specimens from Kryopigi probably belong to male individuals.

INSERT FIGURE 8 AROUND HERE

PCA of the dentition returns a PC1 that explains 32.45% of the variance (horizontal axis of Fig. 9). It is mainly a measure of M^3 posterior breadth. Premolar breadth and M^2 length are the only variables that load negatively on this PC. PC2 explains 17.5% of the variance and is plotted as the vertical axis in Figure 9. It increases mainly with decreasing M^3 length. In Figure 9, the KRY5600 specimen is compared with material of *M. pentelicus* from the type locality and VTK56 from Vathylakkos, which is referred to *M. delsoni/pentelicus* by Koufos (2009) and is considered an intermediate morphotype between the two species. Unfortunately, the upper dentition of *M. delsoni* is not known from the type locality and thus it is not included in the comparison. In Figure 9, males and females from Pikermi show a substantial overlap. The dentition of the Kryopigi specimen lies inside the observed range of males and outside that of females. The Vathylakkos female specimen is located below the Pikermi material in the bivariate distribution and just outside the observed area of *M. pentelicus.* Its separation along the vertical axis is due to the longer third molar. However, it is plotted inside the 95% confidence ellipses of *M. pentelicus*. Moreover, two-group multivariate permutations (n = 2000) with tooth dimensions of C^s-M^2 between males from Kryopigi (KRY2042 and KRY5600) and Pikermi shows that the hypothesis for equal multivariate means cannot be rejected (p = 0.38).

INSERT FIGURE 9 AROUND HERE

4.3. Mandible

Mandibular corpus depth and symphysis dimensions (length and height) distinguish *M. delsoni* from *M. pentelicus* (e.g., Bonis et al., 1990; Koufos 2009a, b). Corpus heights, measured buccally below P_4 and M_3, of male *Mesopithecus* from various localities are compared on a scatter diagram (Figure 10). Specimens from Pikermi and Kalimantsi are intermediate in height compared to those from other localities. Mandibular symphysis height and length (including specimens from various Balkan Turolian localities) are also plotted on a scatter diagram (Figure 11). The symphyseal dimensions of the Kryopigi mandible are similar to those of *M. pentelicus* from Pikermi. In the Kryopigi specimen, the alveolar plane is strongly inclined, the transverse torus is weak, as is the fossa genioglossa, and there is no symphyseal constriction. These characters are similar to those seen in *M. pentelicus* and distinguish it from *M. delsoni*. Table 13 shows a comparison of various Greek *Mesopithecus* mandibles with that of Kryopigi.

INSERT FIGURES 10 & 11 & TABLE 13 AROUND HERE

4.4. Lower dentition

Lower dental dimensions of *Mesopithecus* from various localities are compared with a PCA (Fig. 12). PC1 explains 33.5% of the variance. It is primarily a measure of M_3 length and is negatively correlated with length of the other two molars. All other variables have a positive influence on the axis, apart from the anterior breadth of the first molar, which has a negligible loading. PC2 corresponds to the vertical axis and explains 18.3% of the variance. Scores on this axis increase mainly with decreasing P_3 breadth. Lengths of molars also have a negative influence, whereas all other variables have positive loadings. Each species covers a distinct area on the diagram (Fig. 12). Specimens of *M. monspesulanus* appear below the other two species and seem to be separated by relatively larger breadth of P_3 and possibly larger M_3. *M. delsoni* from Ravin des Zouaves-5 is located to the right side of the diagram and it is separated from *M. pentelicus* along the horizontal axis by its relatively longer M_3 and shorter M_1 and M_2. Furthermore, the specimens from Ravin des Zouaves-5 lie outside the

95% confidence ellipses of both male and female *M. pentelicus* from Pikermi, which means the hypothesis that the Ravin des Zouaves-5 form belongs to this species is rejected. The specimen from Kryopigi is closer to *M. pentelicus* and inside the 95% confidence ellipse of males.

INSERT FIGURE 12 AROUND HERE

4.5. Atlas

The atlas KRY 5600 was compared to a sample of extant colobines (Supplementary Online Material (SOM) and Table S3). The measurements are well within the variation of a modern sample of African and Asian colobines. The dorso-ventral diameter of the vertebral canal is well within the colobine ranges of variation (Table 14 and Fig. 13). Compared to the Asian colobines, it is slightly larger than *Trachypithecus phayrei* and smaller than *Nasalis larvatus* males. The anterior arch shows a well-developed anterior tubercle with a caudal projection. As with the other measures, the size of the anterior arc is well within the colobine modern range of variation (Fig. 14).

INSERT FIGURES 13 & 14 & TABLE 14 AROUND HERE

4.6. Postcrania

The distal humerus fragment is compared with male and female specimens of *M. pentelicus* from Pikermi (Delson 1973; Zapfe 1991), *M.* aff. *delsoni* from Hadjidimovo (Koufos et al. 2003) and *M. pentelicus/delsoni* from Perivolaki (Koufos, 2006) (Fig.15A), although the latter two samples are represented by only female specimens. Figure 15 plots distal epicondylar breadth against the breadth of the trochlea and capitulum. The Kryopigi humerus is similar to male *M. pentelicus* from Pikermi. All of the humeral indices calculated (Table 6) for the new material fall within the ranges of Pikermi *M. pentelicus*, except the ratio of the transverse diameter of the fossa olecrani to the maximum height of trochlea, which is slightly higher for the Kryopigi specimen. It is, however, within two standard deviations of the mean female value for this index, meaning that this difference should not be considered significant. The depth of the fossa olecrani is in the range of *M. pentelicus* from Pikermi (4.8-7.4 mm; Zapfe, 1991). The posteriorly reflected medial epicondyle suggests terrestriality (Delson, 1973) and fits with the known morphology of *M. pentelicus* (Youlatos et al., 2012).

The Kryopigi radius is larger than those of female individuals (e.g., from Hadjidimovo; Koufos et al., 2003) and therefore it likely belonged to a male. The Kryopigi ulna, when compared to specimens from Pikermi (Delson, 1973) and Perivolaki (Fig.15B; Koufos, 2006), is closest to the dimensions of a single male specimen from Pikermi (Delson, 1973). The moderately retroflected olecranon process resembles that of terrestrial cercopithecoids (Delson, 1973; McCrossin et al., 1998). The Kryopigi astragalus (n = 3) has a distally wide and posteriorly tapering trochlea tali, and a well-developed and protruding medial tubercle. The talar head shape and orientation resemble those of other colobines, but are coupled with cercopithecine-like characters, such as a short and robust neck and a well-developed medial malleolar facet, seen in *M. pentelicus* (Delson, 1973; Zapfe, 1991; Youlatos and Koufos, 2010; Alba et al., 2014). Based on size, the astragalus KRY8900 most likely belongs to a male. The rest are smaller and probably represent female individuals. In the bivariate distribution of astragalar length and width (Fig. 15C), the male resembles Pikermi *M. pentelicus* (Zapfe, 1991), whereas the presumed females appear to be narrower than female specimens from Pikermi, Hadjidimovo and Perivolaki (Zapfe, 1991; Koufos et al., 2003; Koufos, 2006). The calcanei are very similar to female specimens of *M. pentelicus* from Pikermi (Fig. 15D).

INSERT FIGURE 15 AROUND HERE

5. Discussion

5.1. Taxonomy

The alpha taxonomy of *Mesopithecus* is currently disputed. There are three species currently recognized in the literature: *M. pentelicus, M. monspessulanus* and *M. delsoni* (e.g., Bonis et al., 1990, Koufos, 2009a, b; Radović et al., 2013). This is the taxonomy followed in this work. Some scholars have proposed additional forms intermediate between these (see Koufos, 2009a, b and references therein). Zapfe (1991), Delson (1994) and Andrews et al. (1996) recognize only the first two species. Rook and Alba (2012) referred all the intermediate forms from Bulgaria and Greece, variously referred to as *M.* cf. *pentelicus*, *M.* aff. *pentelicus*, *M.* cf. *delsoni*, *M.* aff. *delsoni* and *M. delsoni/pentelicus* (see de Bonis et al., 1997; Koufos et al., 2003, 2004; Koufos, 2006, 2009a, b), to *Mesopithecus* sp. More recently, Alba et al. (2015) provisionally distinguished *M. delsoni* at the subspecific level (i.e., *M. p. pentelicus* and *M. p. delsoni*) and all the previously mentioned intermediate forms as *M. pentelicus* subsp. indet.

Andrews et al. (1996) tested the validity of *M. delsoni* by comparing the Pikermian and "Macedonian" populations and concluded that *M. delsoni* cannot be distinguished from *M. pentelicus* even at subspecific level. However, they compared a mixed sample of material from various localities, including Ravin des Zouaves-5, Ravin-X, Titov Veles and Bulgarian sites, some of which have since been allocated to other taxa (e.g., Radović et al., 2013).

Variation between the mandibles from the different sites has been interpreted as species level differences by Bonis et al. (1990) and as taphonomic deformation by Andrews et al. (1996). Zapfe (1991) considered it possible that the *M. delsoni* holotype was instead a male *M. pentelicus*. However, three specimens are known from the type locality of *M. delsoni* (two males and one female), and these show the same characteristics without any substantial deformation (Bonis et al., 1997). Furthermore Bonis et al. (1997) reported that the index of mandibular corpus height below M_2 to tooth row length is higher in *M. delsoni* than in *M. pentelicus*. Delson et al. (2000) argued that *M. delsoni* could not be considered a separate species by virtue of its larger size, compared to *M. pentelicus*. Nevertheless, Koufos et al. (2003) provided further morphological distinctions between the two species based on the Bulgarian sample.

Overall, comparisons of Late Turolian Greco-Iranian *Mesopithecus* cranial, dental and postcranial material favor attribution of the Kryopigi fossils to the species *M. pentelicus*. Regarding morphological characters, such as shape of the fossa genioglossa and anterior symphysis, the Kryopigi specimens are similar or even identical to what is believed to be the pattern in typical *M. pentelicus*.

5.2. Biochronological implications

The present interpretation of the Greek *Mesopithecus* fossil record is strongly dependent on time and suggests that size decreases through the Turolian, as evident from the temporal sequence *M. delsoni* - *M. pentelicus* - *M. monspessulanus* (e.g., Koufos 2008, 2009a, b and references therein). The co-occurrence of the latter two species at Dytiko locality may suggest that these taxa do not represent a simple anagentic lineage. The age of the Kryopigi fauna has been estimated to be between 7.3 and 6.4 Ma, which is consistent with the presence of *M. pentelicus*.

5.3. Taphonomic remarks

The Kryopigi *Mesopithecus* dental material belongs to at least four male individuals, based on the upper right second molars. Among the postcrania, the astragalus is the most numerous (*n* = 3), representing at least one presumed male and one presumed female. Therefore, a minimum of five individuals (MNI: four males and one female) are represented in the collection.

Some of the postcrania, such as the humerus and ulna, were found close to the skull KRY5600, found also with the atlas attached. This is not unusual for the locality, as associated limb elements and mandibles attached to the skulls from other mammals, such as bovids and hipparions, have also been found. This is indicative of limited transportation and fast burial.

The details of the puncture marks on the cranium are typical bite-marks. The shape, size and arrangement of these defects fit with the tooth dimensions and position of a sub-adult individual of the large hyena *Adcrocuta eximia.* This suggests that the predator of this Kryopigi *Mesopithecus* male individual could have been this large Late Miocene hyena, the remains of which predominate among the carnivore material of Kryopigi. Apart from hyenids, Zapfe (1981) also referred to a felid (*Metailurus parvulus*) as predator of *Mesopithecus*, but there is no evidence that this carnivore preyed on *Mesopithecus* at Kryopigi.

5.4. Paleoecological remarks

Mesopithecus occurs in Late Miocene environments that have been interpreted as open and dry, with seasonal climates (Clavel et al., 2012). It probably inhabited slightly wooded landscapes, including a developed grassy herbaceous layer (Clavel et al., 2012) Its diet has been inferred to be based on fruit and seeds (Merceron et al., 2009a, b), and it engaged in both terrestrial and arboreal locomotion (Youlatos, 1999, 2003; Youlatos and Koufos, 2010). It probably inhabited slightly wooded landscapes, including a developed grassy herbaceous layer (Clavel et al., 2012). The configuration of the elbow joint and the shape of the astragalus in the Kryopigi postcrania matches that of terrestrial cercopithecoids (McCrossin et al., 1998; Alba et al., 2014).

6. Conclusions

New cranial, dental and postcranial elements of *Mesopithecus* from Kryopigi, Greece, are described. The fauna suggest that the site dates from between 7.3-6.4 Ma. The presence of associated elements indicates minimal transport and quick burial. The remains represent at least five individuals and both sexes. Although the alpha taxonomy of the genus is currently disputed, detailed morphological, metric and multivariate comparisons of the new material strongly suggest its attribution to *M. pentelicus*. The skull preserves evidence of carnivoran predation.

Acknowledgments

Excavations in Kryopigi have been partly funded by the former Prefecture of Chalkidiki and have been supported by the Municipality of Kassandra. G.L. thanks Prof. G.D. Koufos (Aristotle University of Thessaloniki) for giving access to the material of *M. delsoni* and discussing the Kryopigi specimens, and to Asst. Prof. D. Youlatos for his advice on the metapodials. E.T. and T.C.R. are thankful to Dr A. Dimitriadis, Professor of Medical School (AUTH) for the scans of the skull. Thanks to Drs. R. Portela (NHM-London); E. Gilissen, W. Wendelen (RMCA-Tervuren) and C. Lefèvre (MNHN-Paris) for access to the collections under their care. We would like to thank the Editor, the AE, and the reviewers for very useful comments that have helped to improve this paper. This work benefited from two SYNTHESYS grants from the European Community Research Infrastructure Action (Projects GB-TAF-3674 and BE-TAF-4132). AGO was supported by a Marie Curie Intra- European

Fellowship during part of this work and was also supported by the Spanish Ministerio de Ciencia y Tecnología (Projects: CGL-2015-65387-C3-2-P, MINECO/FEDER). AGO is part of the Research Group IT1044-16 (Gobierno Vasco/Eusko Jaurlaritza) and also funded by the Research Group PPG17/05 (Euskal Herriko Unibertsitatea). The mandible was detached from the skull KRY5600 in the laboratory of the Department of Paleontology of the University of Vienna.

References

Alba, D., Delson, E., Carnevale, G., Colombero, S., Delfino, M., Pavia, M., Pavia, G., 2014. First joint record of *Mesopithecus* and *Macaca* in the Miocene of Europe. Journal of Human Evolution 67, 1–18.

Alba, D.M., Montoya, P., Pina, M., Rook, L., Abella, J., Morales, J., Delson. E., 2015. First record of *Mesopithecus* (Cercopithecidae, Colobinae) from the Miocene of the Iberian Peninsula. Journal of Human Evolution 88, 1–14.

Andrews, P., Harrison, T., Delson, E., Martin, L., Bernor, R.L., 1996. Systematics and biochronology of European and southwest Asian Miocene catarrhines. In: Bernor, R.L., Fahlbusch, V., Mittmann, H.W. (Eds.) Evolution of Western Eurasian Late Neogene Mammal Faunas. Columbia University Press, New York, pp. 168–207.

Bonis, L. de, Bouvrain, G., Geraads, D., Koufos, G., 1990. New remains of *Mesopithecus* (Primates, Cercopithecoidea) from the Late Miocene of Macedonia (Greece), with the description of a new species. Journal of Vertebrate Paleontology 10, 473–483.

Bonis, L. de, Bouvrain, G., Geraads, D., Koufos, G., 1997. New material of *Mesopithecus* (Mammalia, Cercopithecoidea) from the Late Miocene of Macedonia, Greece. Neues Jahrbuch für Geologie und Paläontologie Monatshefte 5, 255–265.

Clavel, J., Merceron, G., Hristova, L., Spassov, N., Kovachev, D., Escarguel, G., 2012. On *Mesopithecus* habitat: Insights from Late Miocene fossil vertebrate localities of Bulgaria. Journal of Human Evolution 63, 162–79.

Delson, E., 1973. Fossil colobine monkeys of the circum-Mediterranean region and the evolutionary history of the Cercopithecidae (Primates, Mammalia). Ph.D. Dissertation, Columbia University.

Delson, E., 1994. Evolutionary history of the colobine monkeys in palaeoenvironmental perspective. In: Davies, A.G., Oates, J.F. (Eds.), Colobine Monkeys: Their Ecology, Behaviour and Evolution. Cambridge University Press, Cambridge, pp. 11–43.

Delson, E., Thomas, H., Spassov, N., 2005. Fossil Old World monkeys (Primates: Cercopithecidae) from the Pliocene of Dorkovo, Bulgaria. Geodiversitas 27, 159–166.

Delson, E., Terranova, C.J., Jungers, W.L., Sargis, E.J., Jablonski, N.G., Dechow, P.C., 2000. Body mass in Cercopithecidae (Primates, Mammalia): estimation and scaling in extinct and extant taxa. Anthropological Papers of the American Museum of Natural History 83, 1–159.

Fortelius, M. (coord.), 2014. New and Old Worlds Database of Fossil Mammals (NOW). University of Helsinki. http://www.helsinki.fi/science/now/.

Gervais, P., 1849. Zoologie et Paleontologie Francaises. A. Bertrand, Paris.

Hammer, Ř., Harper, D.A.T., Ryan, P. D., 2001. PAST: Paleontological Statistics Software Package for Education and Data Analysis. Palaeontologia Electronica 4, 9pp. http://palaeo-electronica.org/2001_1/past/issue1_01.htm

Harrison, T., Delson, E., 2007. *Mesopithecus sivalensis* from the Late Miocene of the Siwaliks . American Journal of Physical Anthropology S44, 126.

Jablonski, N.G., Su, D., Kelly, J., Flynn, L.J., Ji, X., 2011. The Mio-Pliocene colobine monkey, *Mesopithecus*, in China. American Journal of Physical Anthropology 144, 174.

Ji, X., Jablonski, N.G., Su, D.F., Deng, C., Flynn, L.J., You, Y., Kelley, J., 2013. Juvenile hominoid cranium from the terminal Miocene of Yunnan, China. Chinese Science Bulletin 58, 3771-3779.

Klingenberg, C.P., 2011. MorphoJ: an integrated software package for geometric morphometrics. Molecular Ecology Resources 11, 353–357.

Koufos, G.D., 2006. The Late Miocene mammal locality of Perivolaki, Thessaly, Greece. 3. Primates. Palaeontographica Abteilung A 276, 23–37.

Koufos, G.D., 2008. The Miocene cercopithecid primates of Greece. Giornate di Paleontologia, Edizione VIII, 129–131.

Koufos, G.D., 2009a. The Neogene cercopithecids (Mammalia, Primates) of Greece. Geodiversitas 31, 817–850.

Koufos, G.D., 2009b. The genus *Mesopithecus* (Primates, Cercopithecidae) in the Late Miocene of Greece. Bolletino della Società Paleontologica Italiana 48, 157–166.

Koufos, G.D., Spassov, N., Kovatchev, D., 2003. Study of *Mesopithecus* (Primates, Cercopithecidae) from the Late Miocene of Bulgaria. Palaeontographica Abteilung A 269, 39–91.

Koufos, G.D., Bonis, L. de, Kostopoulos, D., Viriot, L., Vlachou, T., 2004. *Mesopithecus* (Primates, Cercopithecoidea) from the Turolian locality of Vathylakkos 2 (Macedonia, Greece). Palaeontologische Zeitschrift 78, 213–228.

Küllmer, O., Doukas, C., 1995. The vertebrate locality of Maramena (Macedonia, Greece) at the Turolian–Ruscinian Boundary (Neogene). 6—The deciduous dentition of *Mesopithecus pentelicus* Wagner (Primates, Mammalia). Münchner Geowissenschaftliche Abhandlungen Reihe A: Geologie und Paläontologie 28, 65–74.

Lazaridis, G., 2010. Contribution to the study of the Neogene Perissodactyla from Kryopigi (Kassandra, Chalkidiki, Greece) (in Greek with English summary). M.S. Thesis, Aristotle University of Thessaloniki.

Lazaridis, G., 2015. Study of the Late Miocene vertebrate locality of Kryopigi and other localities of Kassandra Peninsula, Chalkidiki (Greece). Systematics, taphonomy, paleoecology, biochronology. Ph.D. Dissertation, Aristotle University of Thessaloniki.

Lazaridis, G., Tsoukala E., 2014. *Hipparion phlegrae*, sp. nov. (Mammalia, Perissodactyla): a new species from the Turolian locality of Kryopigi (Kassandra, Chalkidiki, Greece). Journal of Vertebrate Paleontology 34, 164–178.

McCrossin, M.L., Benefit, B.R., Gitau, S.N., Palmer, A.K., Blue, K.T., (1998). Fossil evidence for the origins of terrestriality among Old World higher primates. In: Strasser, E., Fleagle, J., Rosenberger, A.L., McHenry, H., (Eds), Primate Locomotion: Recent Advances, Springer Science & Business Media New York, pp. 353–396.

Marigó, J., Susanna, I., Minwer-Barakat, R., Madurell-Malapeira, J., Moyà-Solà, S., Casanovas-Vilar, I., Robles, J., Alba, D.M., 2014. The primate fossil record in the Iberian Peninsula. Journal of Iberian Geology 40, 179–211.

Merceron, G., Koufos, G.D., Valentin, X., 2009a. Feeding habits of the first European colobine, *Mesopithecus* (Mammalia, Primates): evidence from a comparative dental microwear analysis with modern cercopithecids. Geodiversitas 31, 865–878.

Merceron, G., Scott, J.S., Scott, R.S., Geraads, D., Spassov, N., Ungar, P.S., 2009b. Folivory or fruit/seed predation for *Mesopithecus*, an earliest colobine from the Late Miocene of Eurasia? Journal of Human Evolution 56, 405–416.

Radović, P., Alaburić, S., Marković, Z., Vlastić, S., 2013. New view on the old collection – 'Pikermian fauna' from the vicinity of Veles (f. Republic of Macedonia). Part 1 – Primates. Bulletin of the Natural History Museum 6, 7–29.

Rae, T.C., 2008. Paranasal pneumatization in extant and fossil Cercopithecoidea. Journal of Human Evolution 54, 279–286.

Rae, T.C., Koppe, T., Spoor, F., Benefit, B., McCrossin, M., 2002. Ancestral loss of the maxillary sinus in Old World monkeys and independent acquisition in *Macaca*. American Journal of Physical Anthropology 117, 293–296.

Rook, L., 1999. Late Turolian *Mesopithecus* (Mammalia, Primates, Colobinae) from Italy. Journal of Human Evolution 36, 535–547.

Rook, L., Alba, D.M., 2012. The pioneering paleoprimatologist Charles Immanuel Forsyth Major (1843-1923), and a *Mesopithecus* tooth from an unrecorded locality of Italy (?Casino Basin) in the Basel Naturhistorisches Museum, Switzerland. Bolletino della Società Paleontologica Italiana 51, 1–6.

Syrides, G., 1990. Lithostratigrahic biostraigraphic and paleogeographic study of the Neogene-Quaternary sedimentary deposits of Chakidiki Peninsula, Macedonia, Greece [in Greek]. Ph.D. Dissertation, Aristotle University of Thessaloniki.

Tsoukala, E., Bartsiokas, A., 2008. New *Mesopithecus pentelicus* specimens from Kryopigi, Macedonia, Greece. Journal of Human Evolution 54, 448–451.

Wagner, A., 1839. Fossile Überreste von einem Affenschädel und anderen Säugethierreste aus Griechenland. Gelehrte Anzeiger der Bayerische Akademie der Wissenschaften 38, 301–312.

Youlatos, D., 1999. Etude fonctionnelle multi variée de l'astragale et du calcanéum de *Mesopithecus pentelici*, Wagner 1839 (Cercopithecoidea, Primates). Primatologie 2, 407–420.

Youlatos, D., 2003. Calcaneal features of the Greek Miocene primate *Mesopithecus pentelicus* (Cercopithecoidea: Colobinae). Geobios 36: 229–239.

Youlatos, D., Koufos, G.D., 2010. Locomotor evolution of *Mesopithecus* (Primates: Colobinae) from Greece: evidence from selected astragalar characters. Primates 51, 23–35.

Youlatos, D., Couette, S., Koufos, G.D., 2012. A functional multivariate analysis of *Mesopithecus* (Primates: Colobinae) humeri from the Turolian of Greece. Journal of Human Evolution 63, 219–230.

Zapfe, H., 1981. A skull of *Mesopithecus* with bite marks. Folia Primatologica 35, 248–58.

Zapfe, H., 1991. *Mesopithecus pentelicus* WAGNER aus dem Turolien von Pikermi bei Athen, Odontologie und Osteologie (Eine Documentation). Neue Denkschriften des Naturhistorisches Museum Wien 5, 12–203.

Zelenkov, N., Boev, Z., Lazaridis, G., 2016. A large ergilornithine (Aves, Gruiformes) from the Late Miocene of the Balkan Peninsula. Paläontologische Zeitschrift 90, 145–151.

FIGURE CAPTIONS

Figure 1. A. The Kryopigi *Mesopithecus* excavation site. B. The *Mesopithecus pentelicus* skull KRY5600 in situ and its discovery position (see arrow) in 2006. C. Map of

Geographic distribution of *Mesopithecus pentelicus* in Central and Eastern Europe: 1. Pikermi and Chomateri localities; 2. Kryopigi; 3. Dytiko; 4. Maramena; 5. Kromidovo; 6. Gorna Sushitsa; 7. Kalimantsi; 8. Prevalec and Brce localities; 9. Casino; 10. Brisighella; 11. Wissberg; 12. Baltavar; 13. Polgardi; 14. Hatvan; 15. Grossulovo; 16. Grebeniki. Data from Andrews et al. (1996); Rook (1999); Koufos et al. (2003); Koufos (2008, 2009a, 2009b); Radović et al. (2013). Map modified after Fortelius (2014).

Figure 2. *Mesopithecus* from Kryopigi. Cranium KRY5600. A. Basal, B. Dorsal; C: Lateral left; D: Lateral right; E: Anterior; F: Posterior; G: Occlusal. Arrows in (C) and (D) indicate bite-marks. Scale bar: 50 mm.

Figure 3. *Mesopithecus* from Kryopigi. Mandible KRY5600. A. Occlusal; B. Labial left; C: Skull (cranium and mandible), oblique view; D: Skull lateral left; E: Posterior; F: Lateral right; G: Mandible occlusal. Scale bar: 50 mm.

Figure 4. *Mesopithecus* from Kryopigi. Atlas KRY5600. A. Cranial; B. Caudal; C. Ventral view. Note that the transverse process (asterisk) is eroded ventrally. Note the arc that bridges the articular mass and the transverse process in the ventral view. Scale bar: 10 mm.

Figure 5. *Mesopithecus* from Kryopigi. Postcrania. A. Humerus KRY5620 left distal; A1. Anterior; A2. Posterior; A3. Lateral; A4. Medial view. B. Radius KRY1309 left distal; B1. Anterior; B2. Posterior; B3. Medial (ulnar) view. C. Ulna KRY5621 left proximal, lateral view; D. Astragalus KRY 8900 right; E. Astragalus KRY2772 right; F. Astragalus KRY2773 left; D1, E1, F1. Proximal views; D2, E2, F2. Distal views; G. Calcaneus KRY2771 left; H. Calcaneus KRY2770 right (proximal views); H2. Medial; H3. Distal view; I, J. Proximal metapodial fragments, KRY7868, 7866, dorsal views; K. Distal metapodial KRY7872; L. Distal metapodial KRY7873; K1, L1. Dorsal views. K2, L2.

distal views; M. Proximal phalanx KRY7869; N. Proximal phalanx KRY7867; O. Proximal phalanx KRY7870; P. Proximal phalanx KRY7871. M1, N1, O1, P. Dorsal views. M2, N2, O2. Distal views. Scale bar: 10 mm.

Figure 6. Scatter diagrams of principal component analysis comparing the cranial measurements of *Mesopithecus pentelicus* from Kryopigi (asterisk) with *Mesopithecus* of various Greek and Bulgarian localities: *M.* aff. *delsoni*, Hadjidimovo (triangle) (Koufos et al., 2003); *M. delsoni/pentelicus*, Vathylakkos-2 (VTK) (invert triangle: male) (Koufos et al., 2004); *M. pentelicus* (square: males; solid square: females) from Pikermi (Delson, 1973; Zapfe, 1991); from Kalimantsi (K-333; K-335) (Koufos et al., 2003) and 95% confidence ellipses. Comparative material listed in SOM Table S1.

Figure 7. PCA of GMM analysis of nine craniofacial landmarks (n = 1 for all extant taxa). PC1 is significantly correlated with centroid size and is not illustrated. PC2 plotted against PC3 (7.554% and 7.324% of the total variance, respectively). The two *Mesopithecus* crania (KRY5600 from Kryopigi, M.8947 from Pikermi) are indicated by stars. KRY5600 is situated on the colobine end of PC3 (vertical axis), near M.8947 and the odd-nosed colobines. Landmarks used for geometric morphometric comparisons: 1. Glabella; 2. Alare; 3. Nasospinale; 4. Prosthion; 5. Ectomolare; 6. Zygomaxillare anterior; 7. Orbitale; 8. Frontomalare orbitale; 9. Frontotemporale. Comparative material listed in SOM Table S2.

Figure 8. Scatter diagrams of mesial breadth versus length of M^2 (A) and M^3 (B) (measurements in mm) comparing *Mesopithecus* from Kryopigi (asterisk) with *Mesopithecus* of various Greek and Bulgarian localities: *M.* aff. *delsoni*, Hadjidimovo range and mean values (solid triangle: males) (Koufos et al., 2003); *M. delsoni/pentelicus*, Vathylakkos-2 (VTK) (invert triangle: males; solid diamond: females) (Koufos et al.,

2004); *M. pentelicus*, Kalimantsi range and mean values (square: males; solid square: females), Kromidovo and Gorna Sushitsa (diamond) (Koufos et al., 2003), Pikermi: areas (gray polygons) of males and females; measurements from Zapfe (1991); Maramena (solid circle) (Küllmer and Doukas, 1995).

Figure 9. Scatter diagrams of principal component analysis comparing the upper dentition of *Mesopithecus* from Kryopigi (asterisk) with *Mesopithecus* of various Greek localities: *M. delsoni/pentelicus*, Vathylakkos-2 (VTK) (invert triangle: male, diamond: female) (Koufos et al., 2004); Pikermi: areas (gray polygons) of males and females; measurements from Zapfe (1991) and ellipses of 95% confidence interval. Bi-plot of the variables is displayed on the bottom left of the diagram.

Figure 10. Scatter diagram of corpus buccal depth at P_4 versus that at M_3 (measurements in mm) comparing *Mesopithecus* from Kryopigi (asterisk) with male *Mesopithecus* of various Greek and Bulgarian localities: *M. delsoni*, male Ravin des Zouaves-5 (x) (Bonis et al., 1990; Koufos, 2009); *M.* aff. *delsoni*, (HD-340), Hadjidimovo (solid triangle); Kalimantsi (triangle) (Koufos et al., 2003); *M. delsoni/pentelicus*, Perivolaki (PER) (invert triangle) (Koufos, 2006); *M. pentelicus*, Kalimantsi (square) (Koufos et al., 2003), Pikermi minimum and maximum observations from Delson (1973) (solid circles) and area (gray polygon) of males from Pikermi (Koufos, 2009b: Fig.4b); *M.* cf. *monspessulanus*, Dytiko-2 (Bonis et al., 1990; Koufos, 2009b).

Figure 11. Scatter diagram of symphysis height versus length (measurements in mm) comparing *Mesopithecus* from Kryopigi (asterisk) with *Mesopithecus* of various Greek and Bulgarian localities: *M. delsoni*, male Ravin des Zouaves-5 (x) (Bonis et al., 1990; Koufos, 2009); *M.* aff. *delsoni*, male (HD-339 and 340) and female (HD-341), Hadjidimovo (solid triangle); Kalimantsi (triangle) (Koufos et al., 2003); *M.*

delsoni/pentelicus, female Perivolaki (PER) (solid diamond) and Vathylakkos-2 (VTK) (Koufos et al., 2004; Koufos, 2006); *M. pentelicus*, male (square) and female (solid square) from Kalimantsi (Koufos et al., 2003), Pikermi min and max observations from Delson (1973) (solid circles) and areas (gray polygons) of males and females (Koufos, 2009b: Fig.4b); *M.* aff. *pentelicus*, male, Dytiko-3 (Bonis et al., 1990; Koufos, 2009b).

Figure 12. Scatter diagram of principal component analysis for lower dentition comparing *Mesopithecus* from Kryopigi (asterisk) with *Mesopithecus* of various Greek localities: *M. delsoni*, male Ravin des Zouaves-5 (x) (Bonis et al., 1990; Koufos, 2009); *M. delsoni/pentelicus*, female Perivolaki (PER) (solid diamond) and Vathylakkos-2 male (diamond) (VTK) (Koufos et al., 2004; Koufos, 2006); Pikermi areas (gray polygons) of males and females from Koufos (2009b: Fig.4b).

Figure 13. Canal dorso-ventral diameter (in mm) of the *Mesopithecus* atlas KRY5600 (solid triangle) compared to other colobines. Note that its size is well within the modern colobine range of variation. Comparative material listed in SOM Table S3.

Figure 14. Bivariate plot (dimensions in mm) of the anterior arc of the *Mesopithecus* atlas KRY5600 (solid triangle) compared to other colobines. Comparative material listed in SOM Table S3.

Figure 15. Scatter diagrams of postcranial bones (A. Humerus, B. Ulna, C. Astragalus, D. Calcaneus) comparing *Mesopithecus* from Kryopigi (asterisk) with *M.* aff. *delsoni*, female, Hadjidimovo (solid triangle); *M. delsoni/pentelicus*, female Perivolaki (PER) (diamond) (Koufos, 2006); *M. pentelicus* (gray polygons) of males (square) and females (solid square) (Delson, 1973; Zapfe, 1991).


A
fossiliferous horizon
1 m
B
C
11
15
14
16
12
13
10
9
7
8
6
5
4
3
2
1

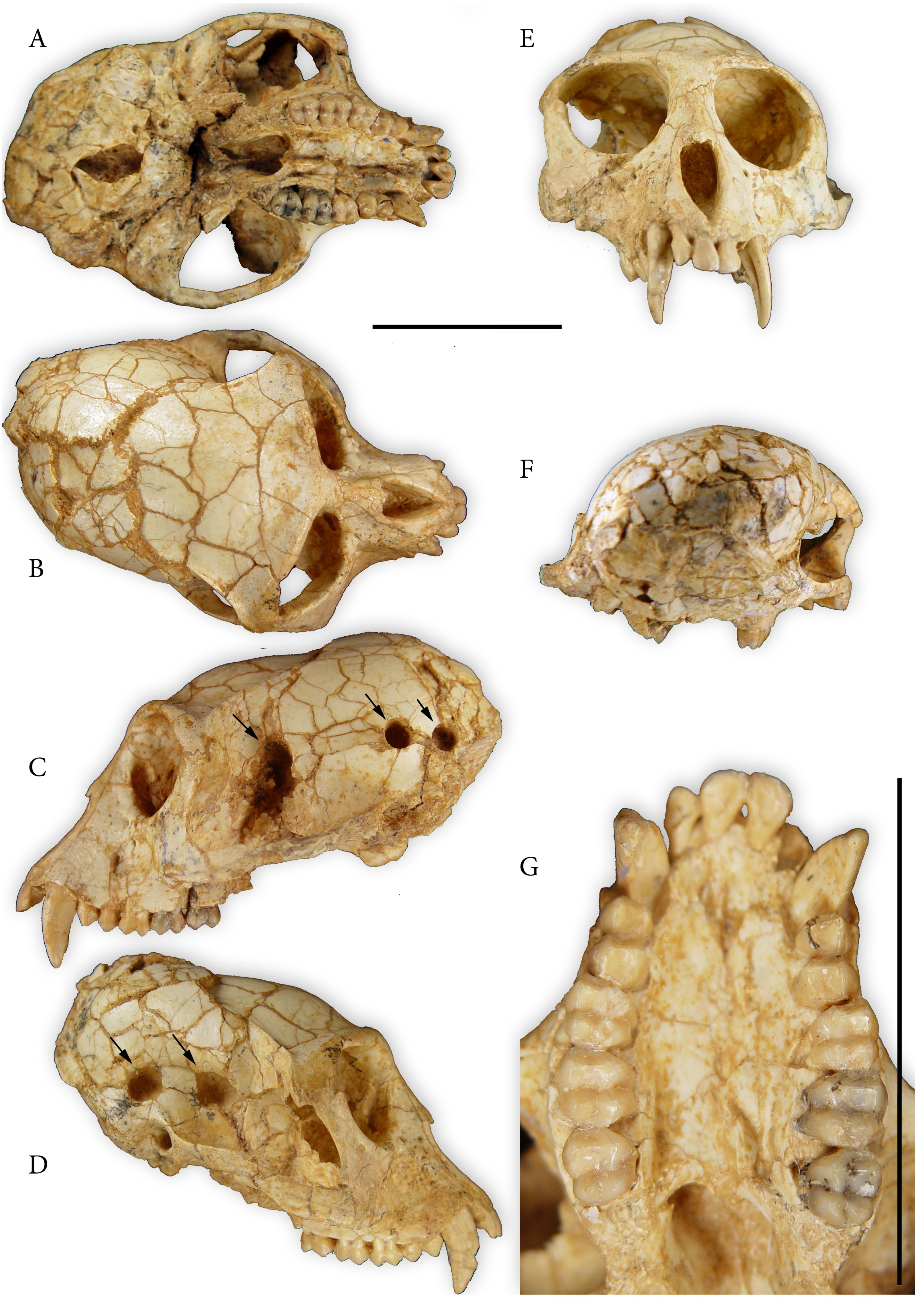
A
B
C
D
E
F
G

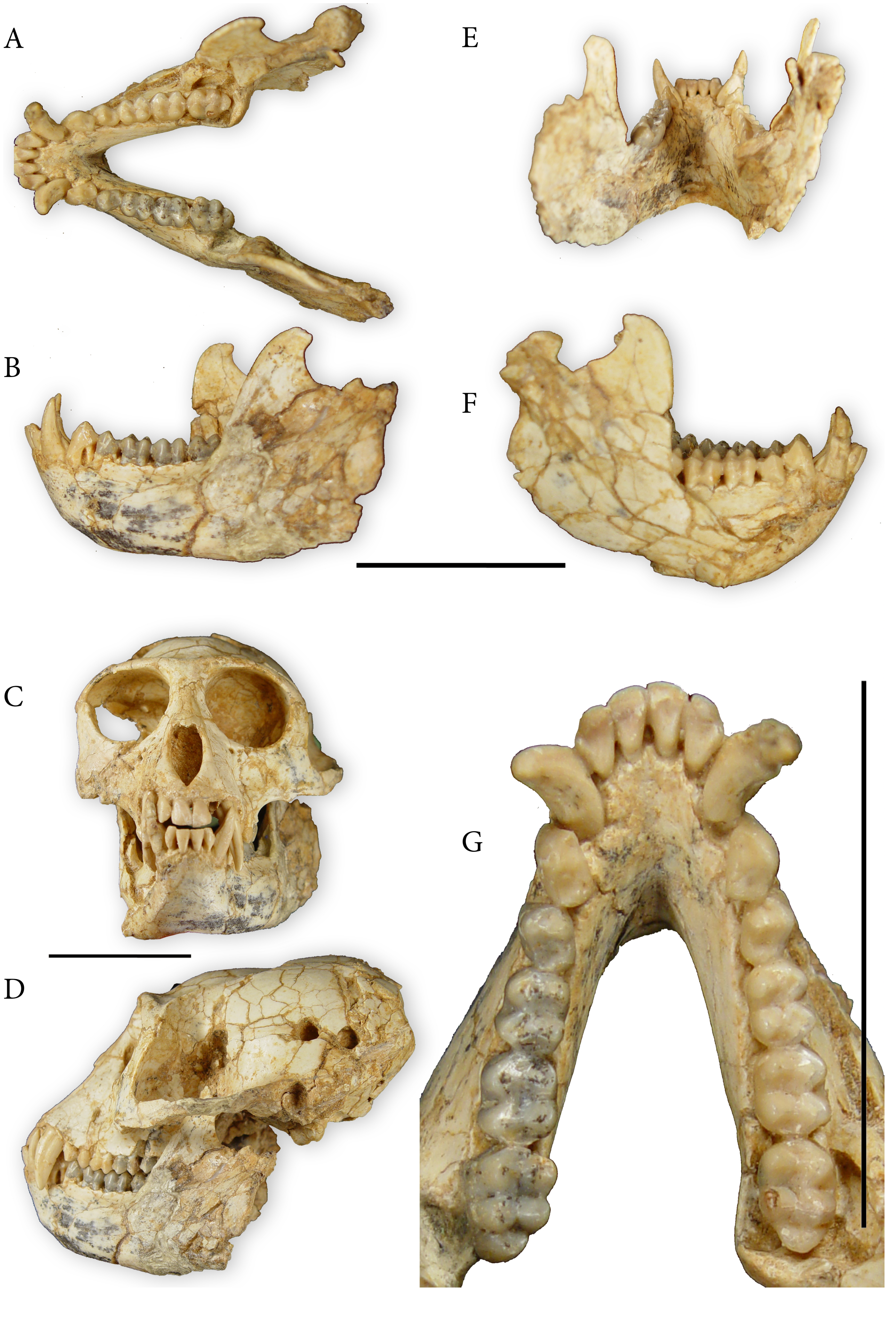
A
B
C
D
E
F
G

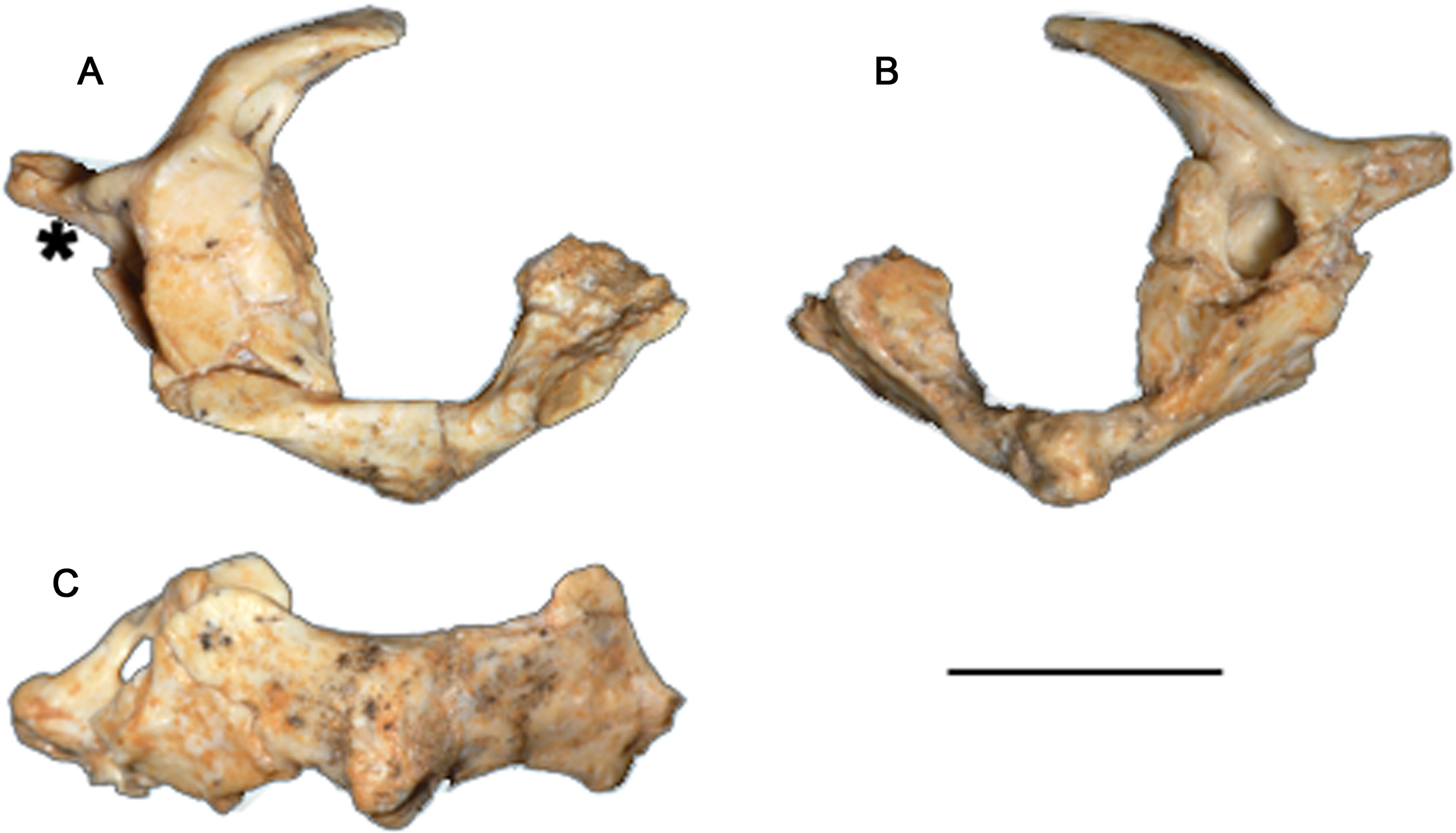
A
B
C
*

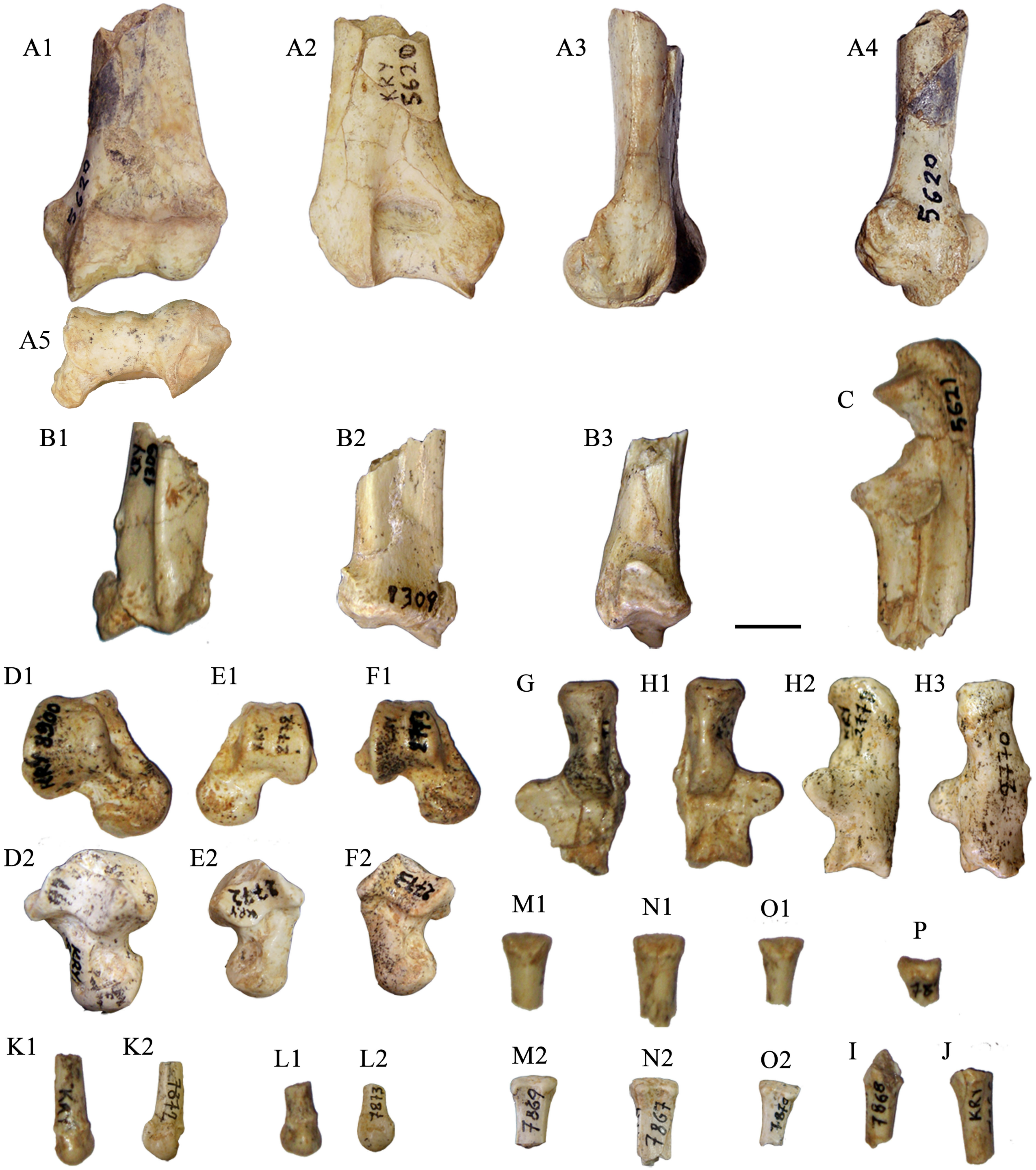
A1
A2
A3
A4
A5
B1
B2
B3
C
D1
E1
F1
G
H1
H2
H3
D2
E2
F2
M1
N1
O1
P
K1
K2
L1
L2
M2
N2
O2
I
J

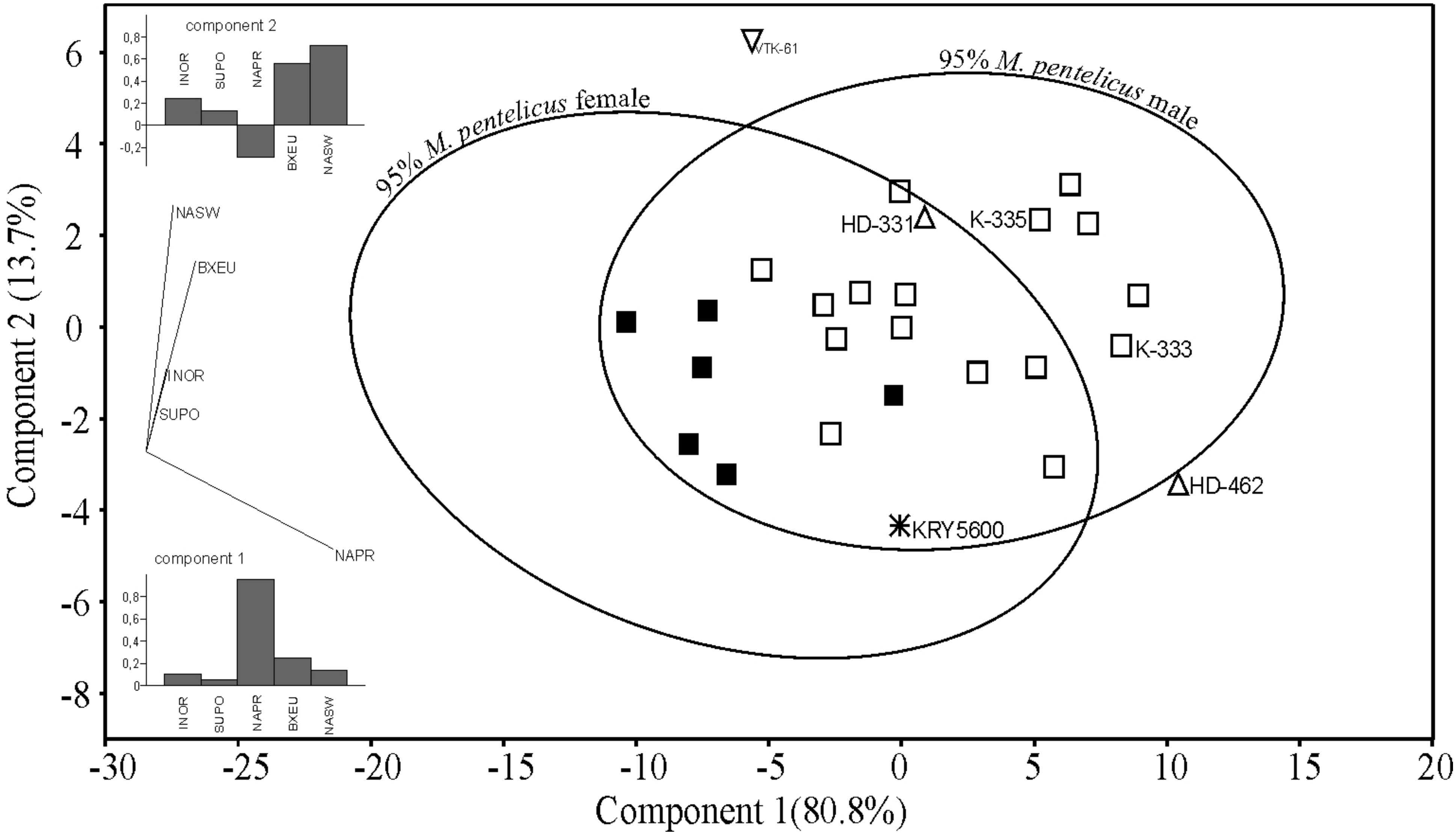

component 2
INOR
SUPO
NAPR
BXEU
NASW
component 1
NASW
BXEU
INOR
SUPO
NAPR
VTK-61
95% M. pentelicus female
95% M. pentelicus male
HD-331
K-335
K-333
HD-462
KRY5600
Component 2 (13.7%)
Component 1(80.8%)

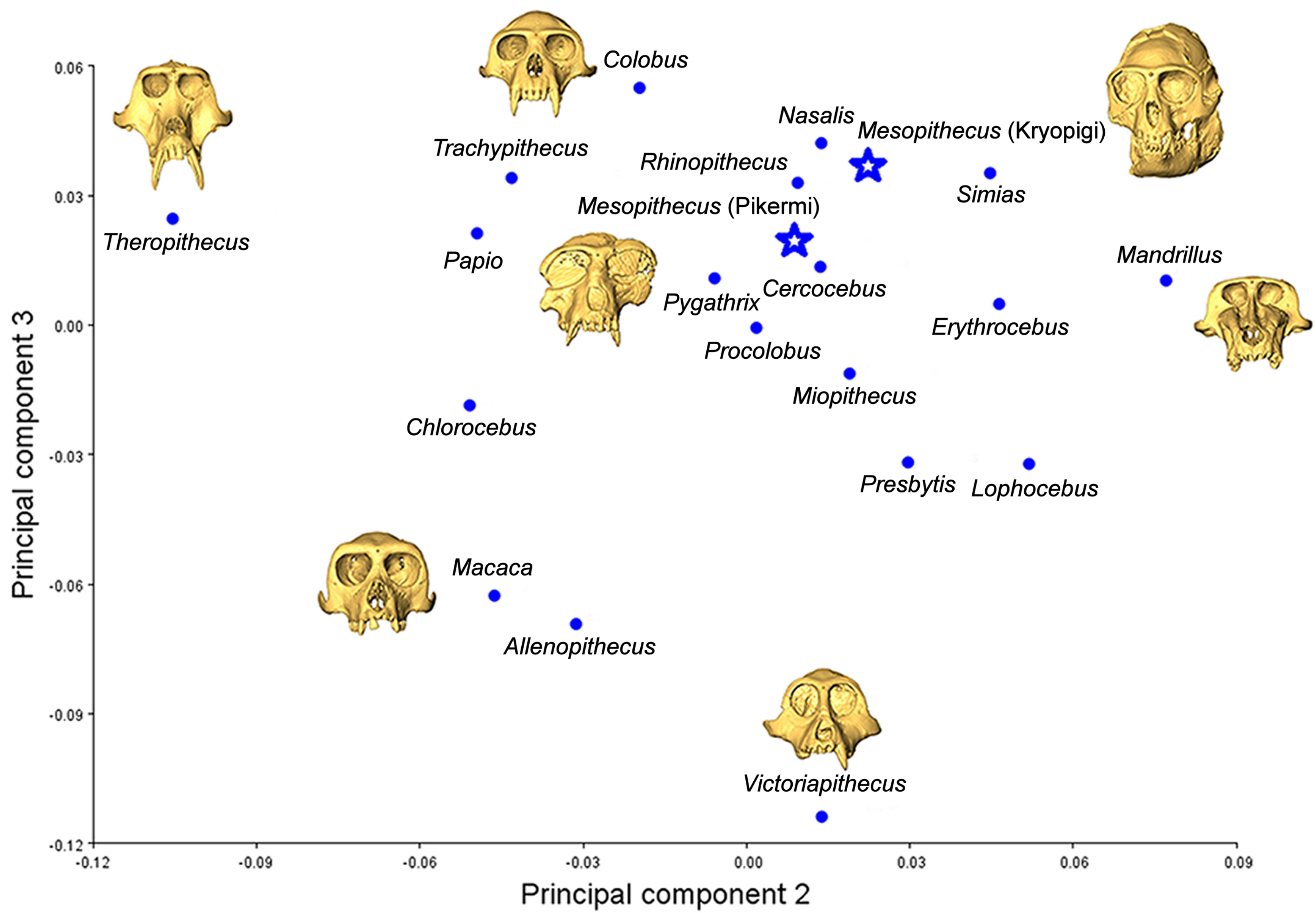

Colobus
Nasalis
Mesopithecus (Kryopigi)
Trachypithecus
Rhinopithecus
Simias
Theropithecus
Mesopithecus (Pikermi)
Papio
Mandrillus
Cercocebus
Pygathrix
Erythrocebus
Procolobus
Miopithecus
Chlorocebus
Presbytis
Lophocebus
Macaca
Allenopithecus
Victoriapithecus
0.06
0.03
0.00
-0.03
-0.06
-0.09
-0.12
-0.12
-0.09
-0.06
-0.03
0.00
0.03
0.06
0.09
Principal component 3
Principal component 2

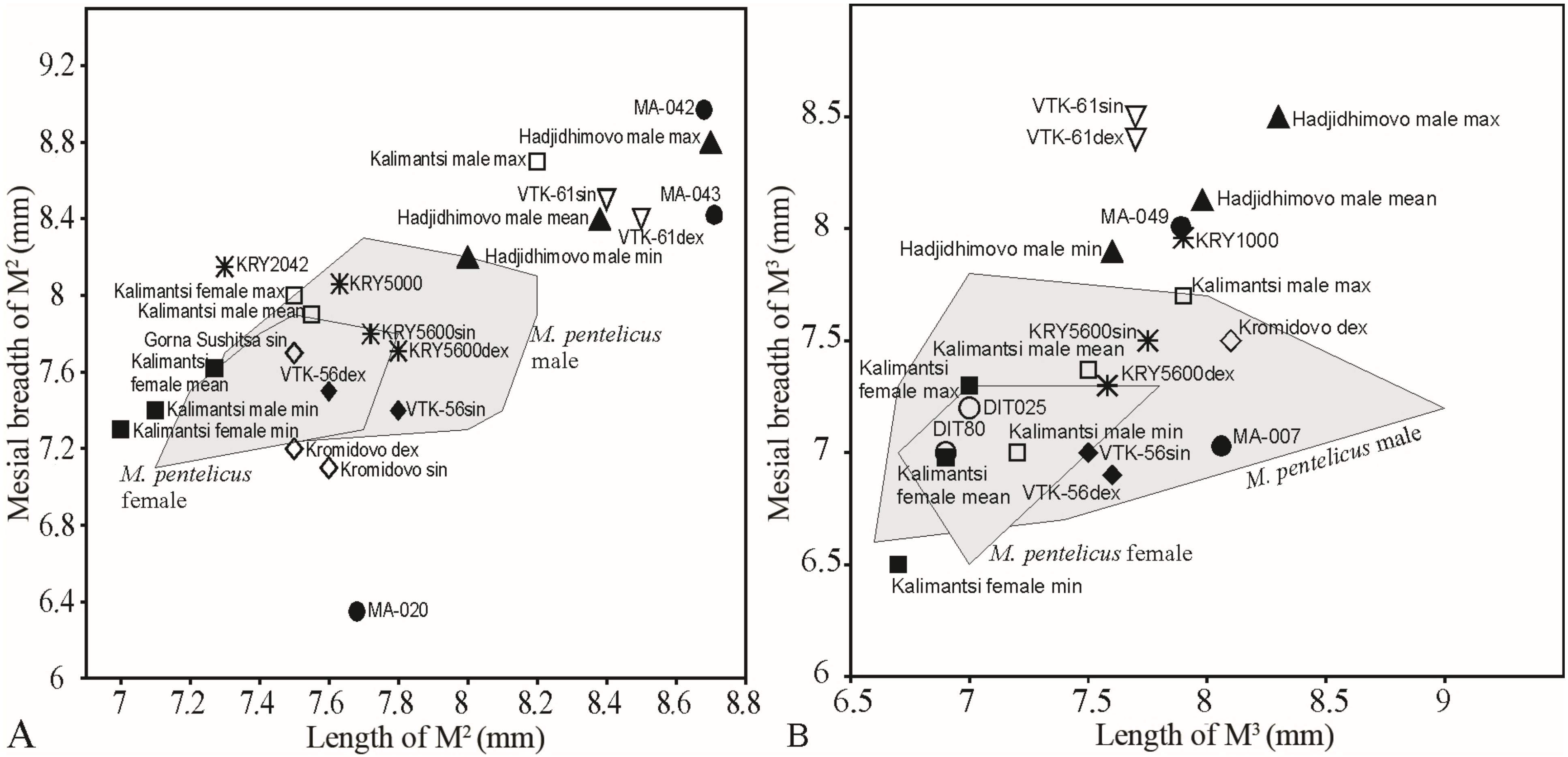
A
Mesial breadth of M² (mm)
Length of M² (mm)
MA-042
Hadjidhimovo male max
Kalimantsi male max
VTK-61sin
MA-043
Hadjidhimovo male mean
VTK-61dex
KRY2042
Hadjidhimovo male min
KRY5000
Kalimantsi female max
Kalimantsi male mean
KRY5600sin
KRY5600dex
M. pentelicus male
Gorna Sushitsa sin
Kalimantsi female mean
VTK-56dex
Kalimantsi male min
VTK-56sin
Kalimantsi female min
Kromidovo dex
Kromidovo sin
M. pentelicus female
MA-020
B
Mesial breadth of M³ (mm)
Length of M³ (mm)
VTK-61sin
VTK-61dex
Hadjidhimovo male max
Hadjidhimovo male mean
MA-049
KRY1000
Hadjidhimovo male min
Kalimantsi male max
KRY5600sin
Kromidovo dex
Kalimantsi male mean
Kalimantsi female max
KRY5600dex
DIT025
DIT80
Kalimantsi male min
MA-007
VTK-56sin
M. pentelicus male
Kalimantsi female mean
VTK-56dex
M. pentelicus female
Kalimantsi female min

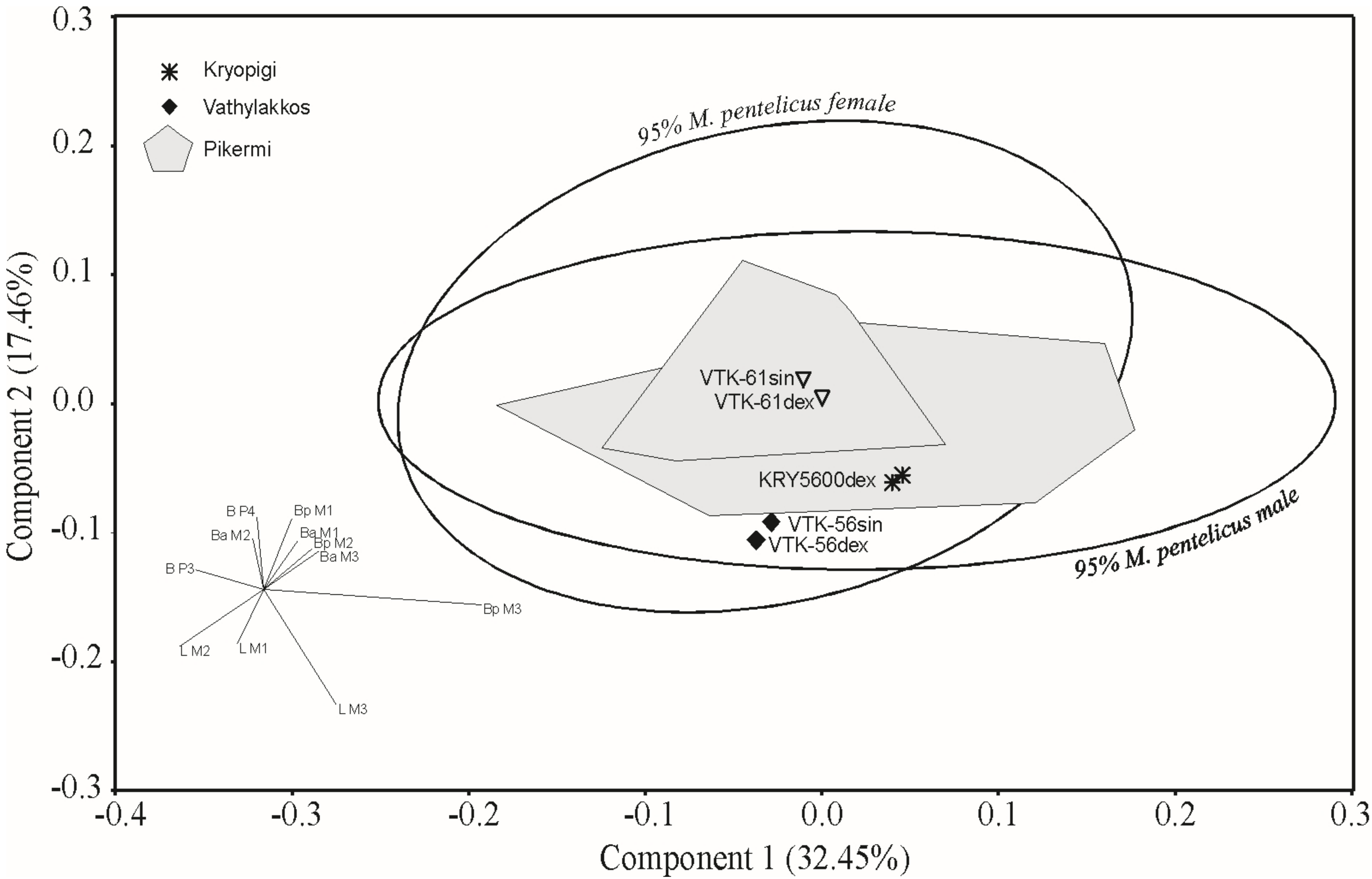
Kryopigi
Vathylakkos
Pikermi
95% M. pentelicus female
95% M. pentelicus male
VTK-61sin
VTK-61dex
KRY5600dex
VTK-56sin
VTK-56dex
B P4
Bp M1
Ba M2
Ba M1
Bp M2
Ba M3
B P3
Bp M3
L M2
L M1
L M3
Component 2 (17.46%)
Component 1 (32.45%)
0.3
0.2
0.1
0.0
-0.1
-0.2
-0.3
-0.4
-0.3
-0.2
-0.1
0.0
0.1
0.2
0.3

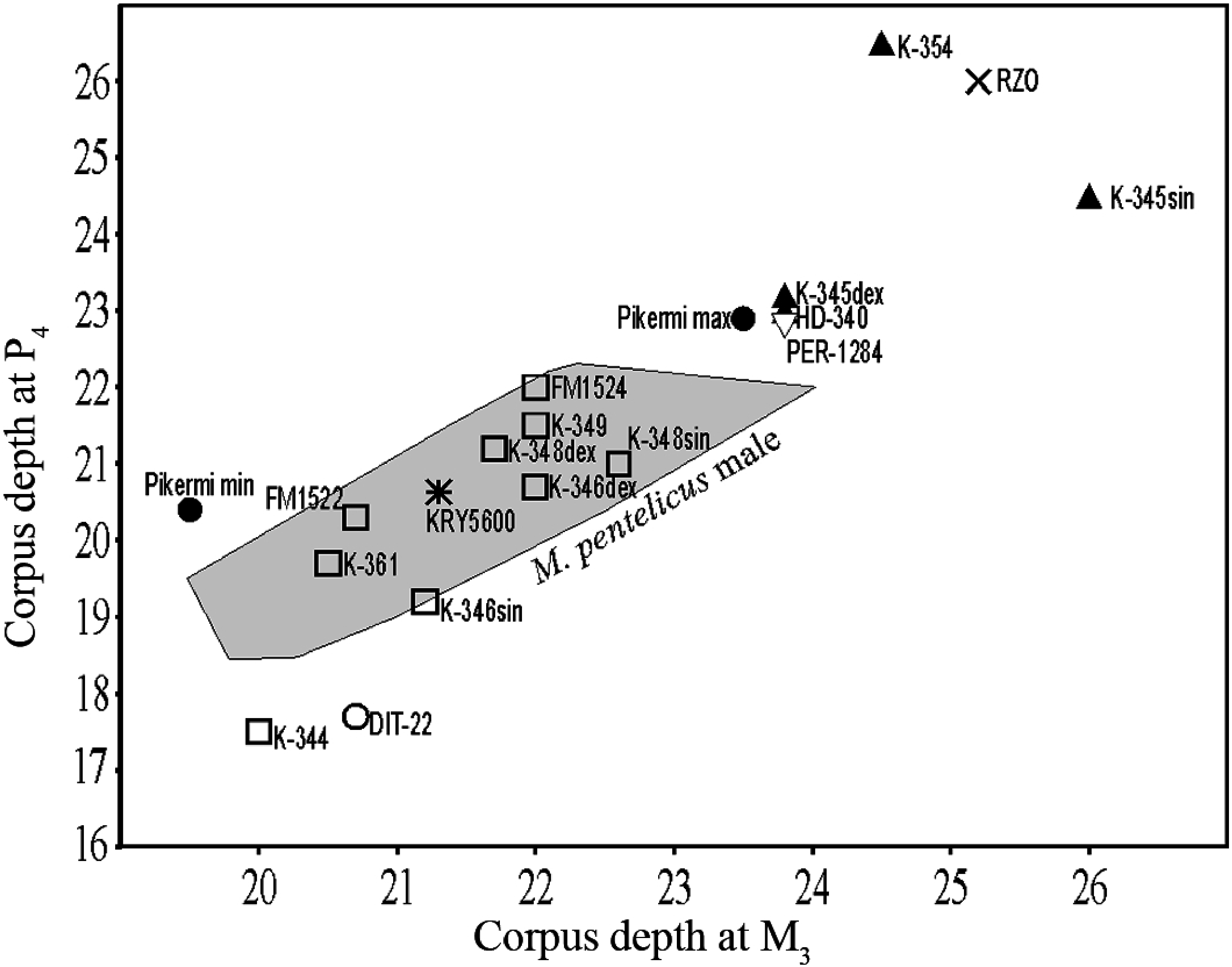

K-354
RZO
K-345sin
K-345dex
Pikermi max
HD-340
PER-1284
FM1524
K-349
K-348sin
K-348dex
K-346dex
Pikermi min
FM1522
KRY5600
M. pentelicus male
K-361
K-346sin
K-344
DIT-22
Corpus depth at P_4
Corpus depth at M_3

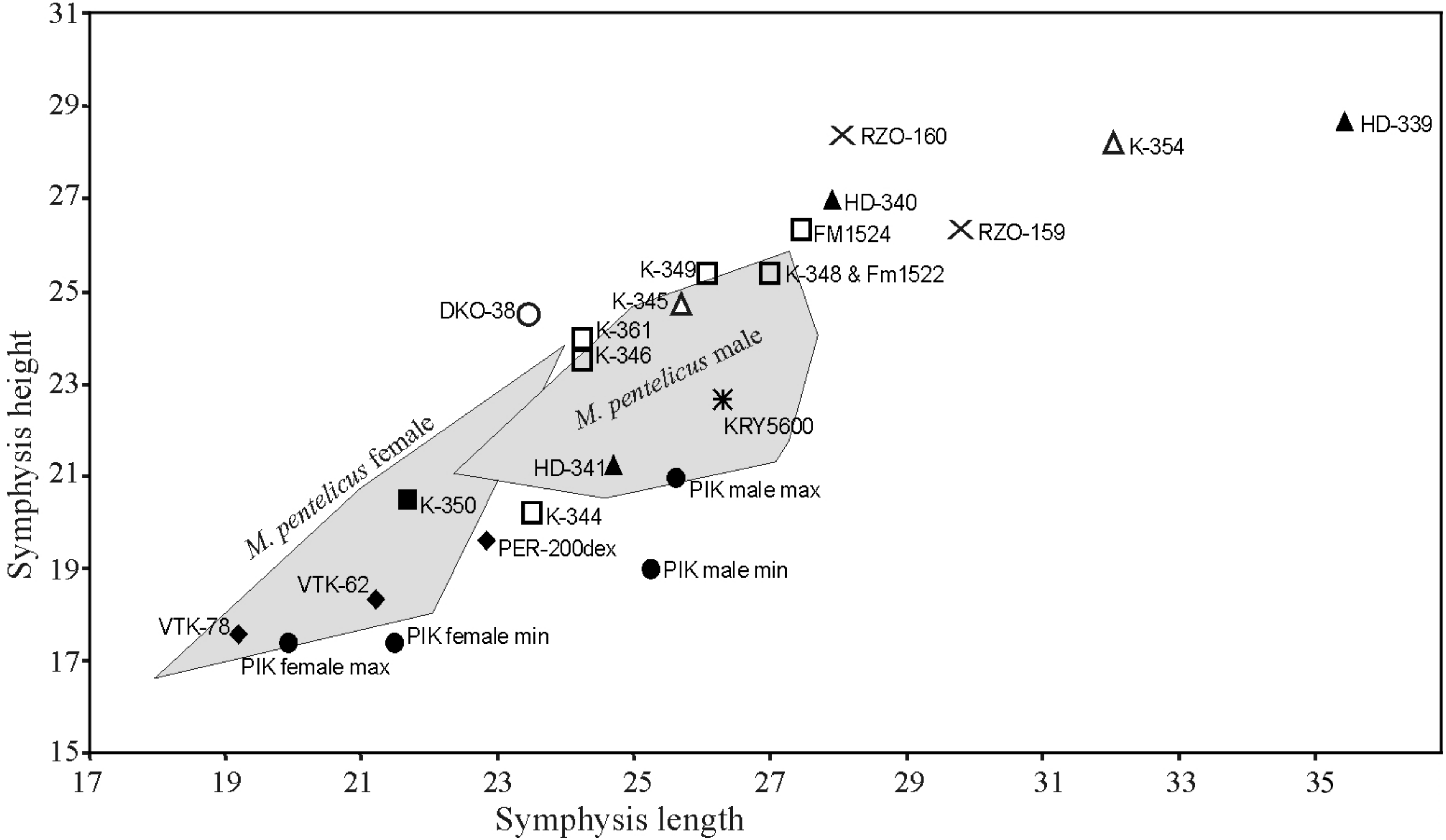

Symphysis height
Symphysis length
31
29
27
25
23
21
19
17
15
17
19
21
23
25
27
29
31
33
35
M. pentelicus female
M. pentelicus male
HD-339
K-354
RZO-160
HD-340
FM1524
RZO-159
K-349
K-348 & Fm1522
K-345
DKO-38
K-361
K-346
KRY5600
HD-341
PIK male max
K-350
K-344
PER-200dex
PIK male min
VTK-62
VTK-78
PIK female min
PIK female max

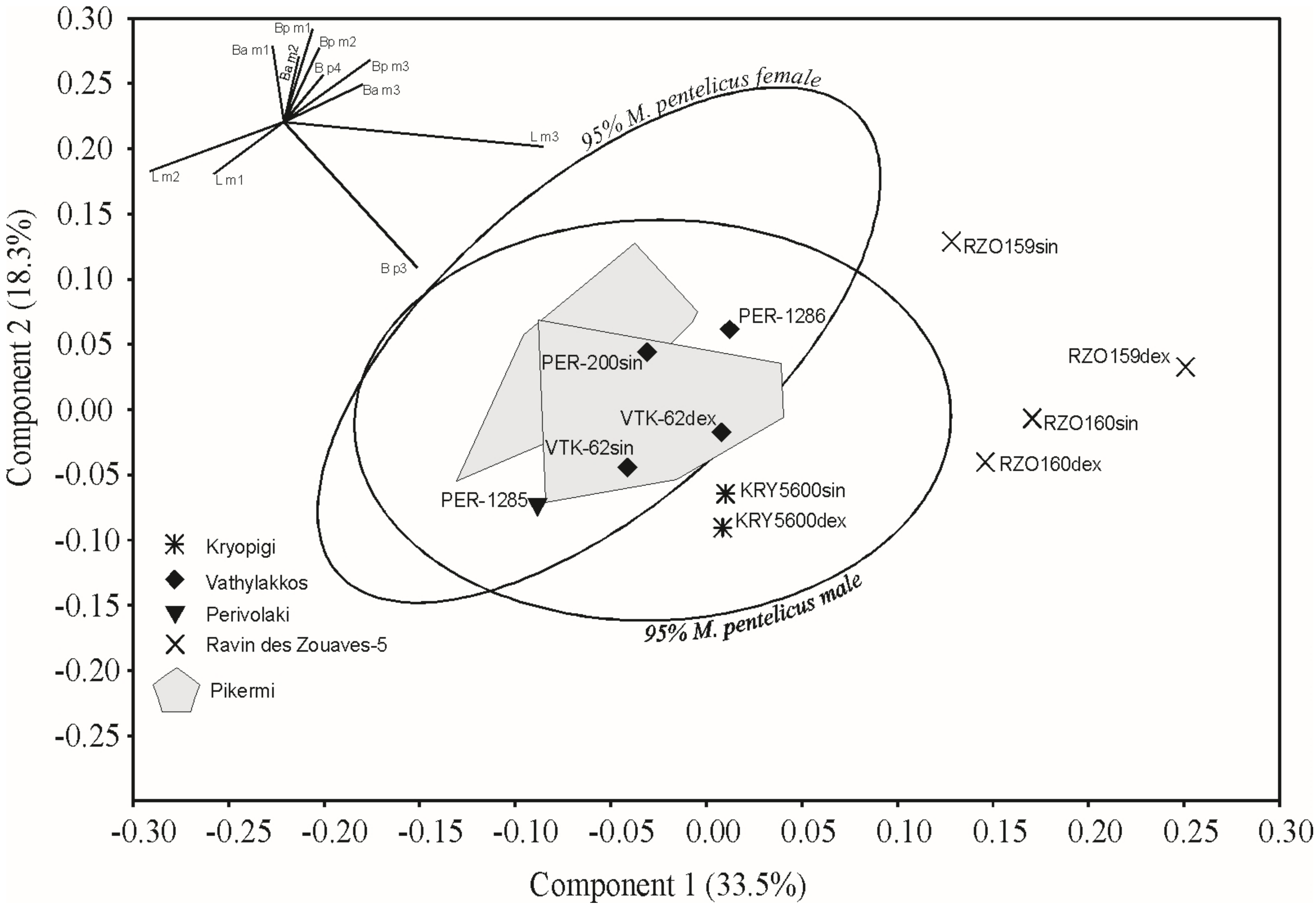

0.30
0.25
0.20
0.15
0.10
0.05
0.00
-0.05
-0.10
-0.15
-0.20
-0.25
Component 2 (18.3%)
-0.30
-0.25
-0.20
-0.15
-0.10
-0.05
0.00
0.05
0.10
0.15
0.20
0.25
0.30
Component 1 (33.5%)
Bp m1
Ba m1
Ba m2
Bp m2
B p4
Bp m3
Ba m3
L m3
L m2
L m1
B p3
95% M. pentelicus female
95% M. pentelicus male
RZO159sin
RZO159dex
RZO160sin
RZO160dex
PER-1286
PER-200sin
VTK-62dex
VTK-62sin
PER-1285
KRY5600sin
KRY5600dex
Kryopigi
Vathylakkos
Perivolaki
Ravin des Zouaves-5
Pikermi

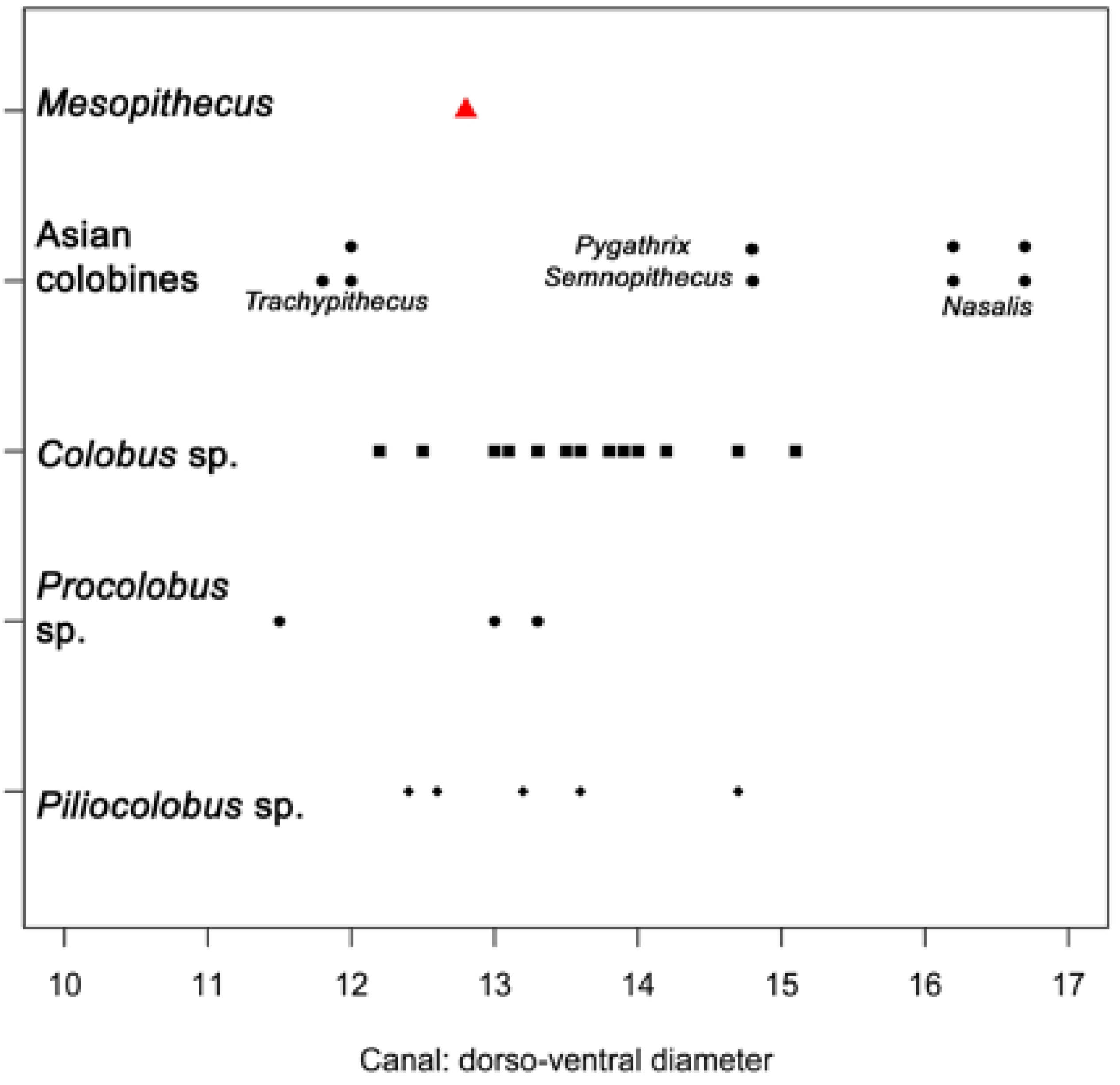
Mesopithecus
Asian colobines
Pygathrix
Semnopithecus
Trachypithecus
Nasalis
Colobus sp.
Procolobus sp.
Piliocolobus sp.
10
11
12
13
14
15
16
17
Canal: dorso-ventral diameter

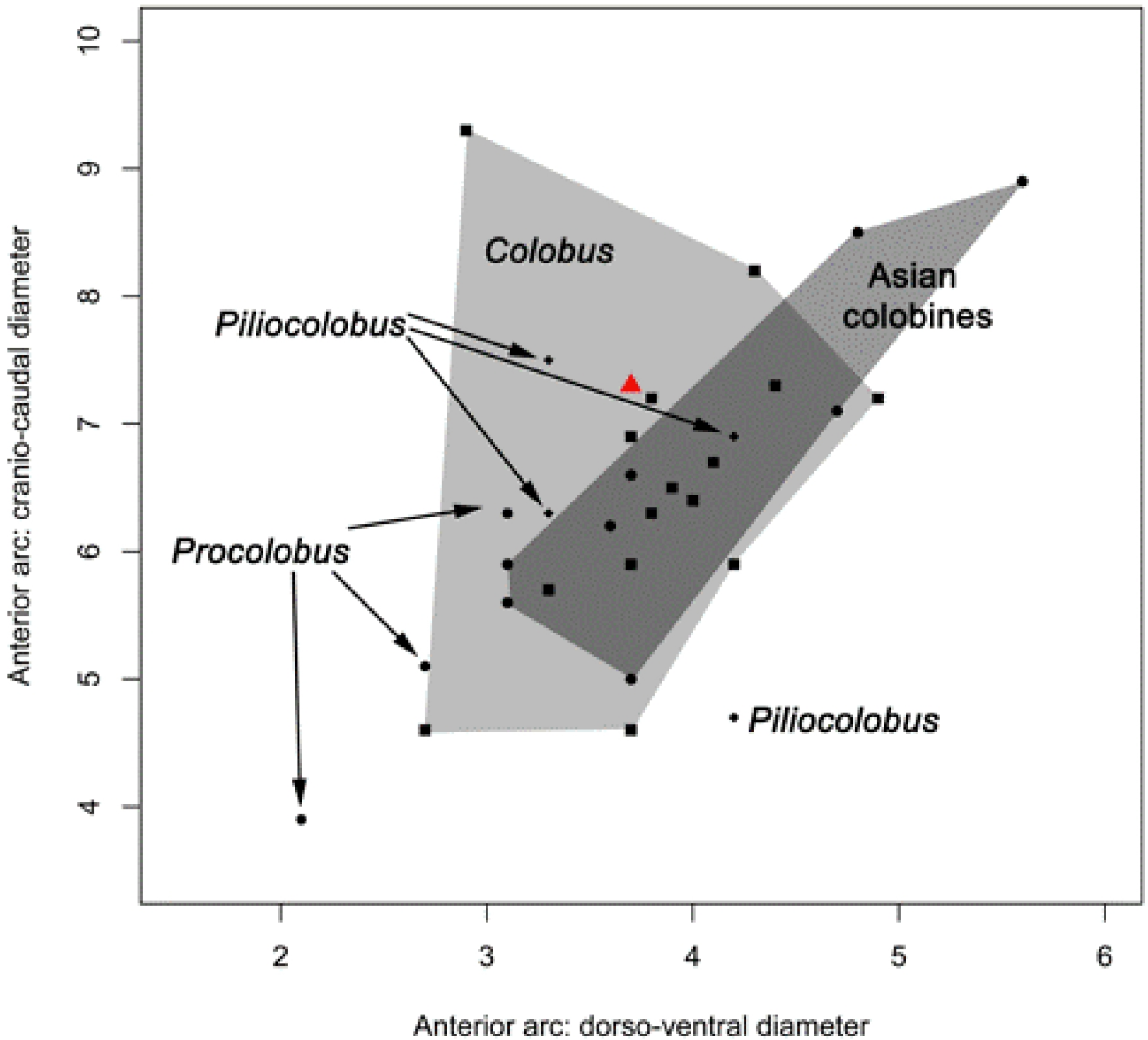
Colobus
Asian colobines
Piliocolobus
Procolobus
Piliocolobus
10
9
8
7
6
5
4
2
3
4
5
6
Anterior arc: cranio-caudal diameter
Anterior arc: dorso-ventral diameter

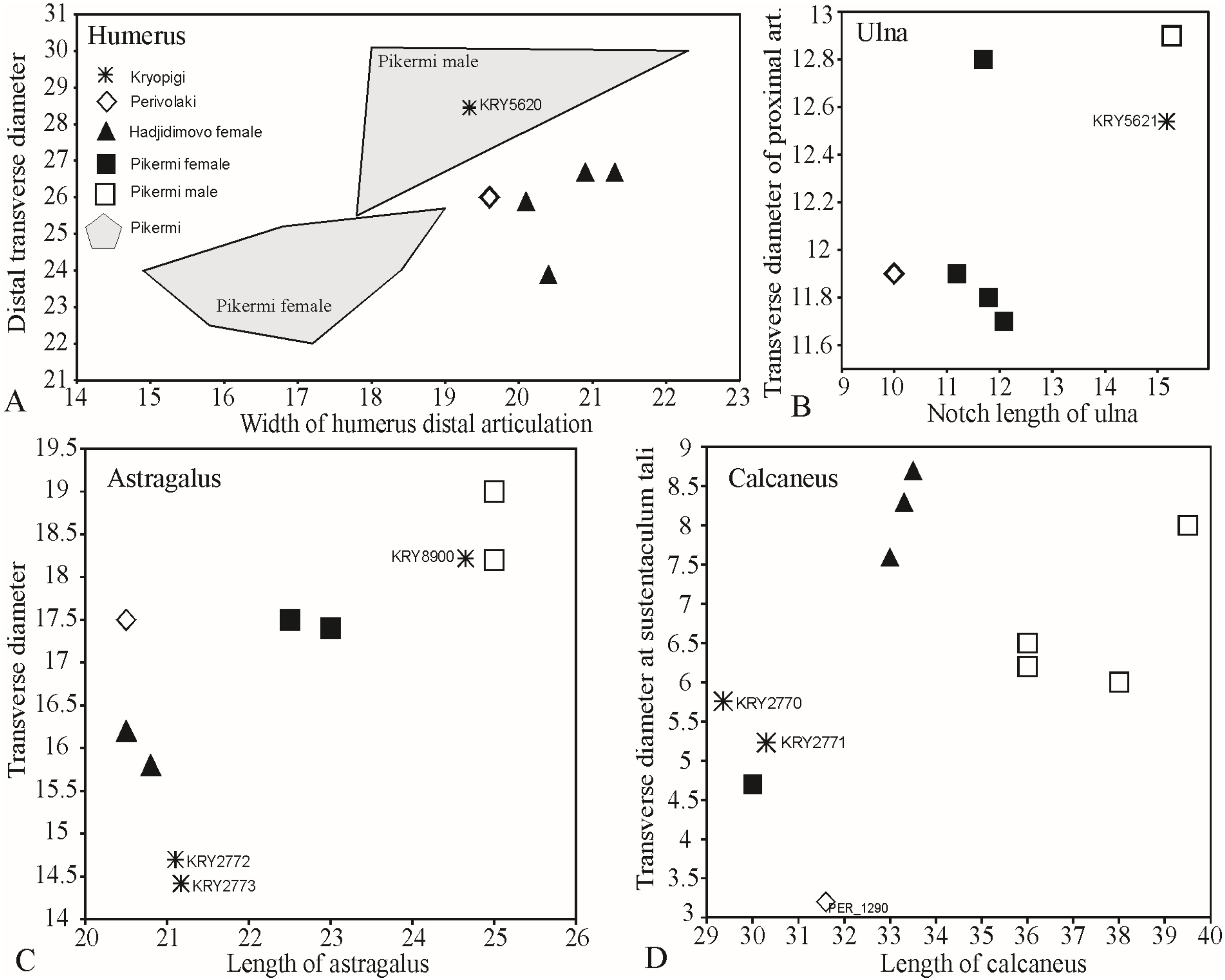

Humerus
Kryopigi
Perivolaki
Hadjidimovo female
Pikermi female
Pikermi male
Pikermi
Pikermi male
KRY5620
Pikermi female
Distal transverse diameter
Width of humerus distal articulation
A
Ulna
KRY5621
Transverse diameter of proximal art.
Notch length of ulna
B
Astragalus
KRY8900
KRY2772
KRY2773
Transverse diameter
Length of astragalus
C
Calcaneus
KRY2770
KRY2771
PER_1290
Transverse diameter at sustentaculum tali
Length of calcaneus
D

Table 1
Faunal list of Kryopigi locality (Lazaridis, 2015; Zelenkov et al., 2015).

Primates	*Hippopotamodon major* (Gervais, 1848-1852)
Mesopithecus pentelicus Wagner, 1839	*Gazella pilgrimi* Bohlin, 1935
Carnivora	*Gazella capricornis* (Wagner, 1848)
Adcrocuta eximia (Roth and Wagner, 1854)	*Prostrepsiceros axiosi* n. ssp.
Hyaenictitherium wongii (Zdansky, 1924)	*Nisidorcas planicornis* (Pilgrim, 1939)
Plioviverops orbignyi (Gaudry and Lartet, 1856)	*Helladorcas* sp.
Amphimachairodus giganteus (Wagner, 1848)	*Skoufotragus* sp.
"Metailurus parvulus" (Hensel, 1862)	*Tragoportax amalthea* (Roth & Wagner, 1854)
cf. *Promephitis larteti* (Gaudry, 1862-1867)	?*Miotragocerus* sp.
Mustelidae indet.	Bovidae indet.
Proboscidea	**Rodentia**
Choerolophodon pentelici Gaudry and Lartet, 1856)	Muridae indet.
Perissodactyla	*Hystrix primigenia* (Wagner, 1848)
cf. *Hippotherium brachypus* (Hensel, 1862)	**Lagomorpha**
Cremohipparion aff. *nikosi*	Lagomorpha indet.
?Cremohipparion sp.	**Reptilia**
Hipparion phlegrae Lazaridis and Tsoukala, 2014	*Varanus* sp.
Artiodactyla	Chelonia indet. (large terrestrial species)
Helladotherium duvernoyi (Gaudry and Lartet, 1856)	**Aves**
Palaeotragus rouenii Gaudry, 1861	*?Amphipelargus* sp.
Propotamochoerus n. sp.	

Table 2
Inventory, description and sex determination of the *Mesopithecus pentelicus* fossils from Kryopigi.

Label	Individual	Sex	Anatomical region	Description	Figure
KRY5600*	1	Male	Cranium	Preserves the right I^{1-2}, C^s, P^2-M^3, and the left I^1, C, P^2-M^3. The cranium shows puncture marks on both side (see text). These could have been produced by the large Late Miocene hyena *Adcrocuta eximia.*	Figures 2-3
	1	Male	Mandible	Preserves right and left I_{1-2}, C_i, P_2-M_3	Figure 3
	1	Male	Atlas (C1)	Anterior arch, right lateral mass and transverse process and part of the posterior arch	Figure 4
KRY2042	2	Male	Right maxilla (fragment)	Preserves C^s-M^2 and the roots of I^2 and M^3	
KRY3462			Left C^s		
KRY7865			Left C^s		
KRY1000	3	Male	Right M^2		
KRY5000	4	Male	Right M^2		
KRY5620[#1]		Male	Left humerus	Distal fragment	Figure 5
KRY5621[#1]		Male	Left ulna	Proximal fragment	Figure 5
KRY1309		Male	Left radius	Distal fragment	Figure 5
KRY8900		Male	Right astragalus	Complete	Figure 5
KRY2773	5	Female	Right astragalus	Complete	Figure 5
KRY2772		Female	Left astragalus	Complete	Figure 5
KRY2770		Female	Right calcaneus	Complete	Figure 5
KRY2771		Female	Left calcaneus	Complete	Figure 5
KRY7866			Metapodial	Shaft fragment	Figure 5
KRY7868			Metapodial	Proximal fragment	Figure 5
KRY7872			Metapodial	Distal fragment	Figure 5
KRY7873			Metapodial	Distal fragment	Figure 5
KRY7867			First phalanx	Proximal fragment	Figure 5
KRY7869			First phalanx	Proximal fragment	Figure 5
KRY7870			First phalanx	Proximal fragment	Figure 5
KRY7871			First phalanx	Proximal fragment	Figure 5

*This specimen represents the skull (both cranium and mandible) and atlas of a male specimen that were found articulated.
[#1]These specimens likely belong to the same individual.

Table 3
Mesopithecus pentelicus KRY: measurements of the cranium (in mm unless stated differently).

Delson, 1973	Measurement		KRY5600
NAIN	Nasion-Inion		84.1
GLIN	Glabella-Inion		82.1
NABA	Nasion-Basion		59.0
GLBA	Glabella-Basion		60.5
NABR	Nasion-Bregma		51.0
NAPR	Nasion-Prosthion		39.0
GLPR	Glabella-Prosthion		46.5
NARH	Nashion-Rhinion		14.6
BAIN	Basion-Inion		27.7
BABR	Basion-Bregma		48.2
BAVE	Basion-Vertex		[50.5]*
BAPR	Basion-Prosthion		75.5
BAST	Basion-Staphylion		36.5
BAPT	Basion-Palate Rear		[38.3]*
PRIN	Prosthion-Inion		111.8
PRST	Prosthion-Staphylion		40.4
PRPT	Prosthion-Palate Rear		38.5
PROB	Prosthion-Orbit Base	right	35.7
PROB	Prosthion-Orbit Base	left	34.9
ZMOB	Zygomaxillary Suture-Orbit Base	right	17.9
ZMOB	Zygomaxillary Suture-Orbit Base	left	16.4
ZMPG	Zygomaxillary Suture-Post Glenoid	right	40.5
ZMPG	Zygomaxillary Suture-Post Glenoid	left	43.7
MAXW	Max. Width (excl. zyg. arches) under auditory region		58.4
FACH	Face Height	right	45.2
FACH	Face Height	left	45.7
TMIN	Min. Width between Temp. Lines		28.0
NATM	Nasion-Midl. Proj. at TMIN		56.3
TMPO	Min. Width Between Temp. lines at PORB		43.6
PORB	Min. Postorbital Width		46.7
BIOR	Max. Bi-Orbital Width		67.1
INOR	Interorbital Width		9.8
ORBH	Orbit Height	right	21.5
ORBH	Orbit Height	left	22.7
ORBW	Orbit Width	right	23.7
ORBW	Orbit Width	left	25.3
SUPO	Supra-Orbital Thickness	right	3.7
SUPO	Supra-Orbital Thickness	left	3.6
FORW	Foramen Magnum Width	compressed	10.8
FORL	Foramen Magnum Length		17.0
NPAP	Proj. of Napr Onto Alv. Plane		25.0
ORHF	Orbit Base-Alv. Plane Height in Frank. Pl.	right	21.1
ORHF	Orbit Base-Alv. Plane Height in Frank. Pl.	left	20.4
BPFP	Length Segment BAPR Ant. ORPH		21.6
ORHA	Orbit Base-Alv. Plane Height at Occl. Plane Horiz.	right	22.0
ORHA	Orbit Base-Alv. Plane Height at Occl. Plane Horiz.	left	20.9
OPAP	Segment of Occl. Length I^1-M^3		24.7
RHNW	Width Nasals at Rhinion		10.4
NASW	Nasal Aperture Max. Width		8.3
NASL	Nasal Aperture Max. Length		22.2
PRND	Prosthion-Inf. End Nasal Aperture		5.6
MHCP	Muzzle Height		16.6
BXEU	Palate Max. Breadth		34.1
I1AU	Breadth Across I^1-I^1		8.2

M3CU	Toothrow Length C^s-M^3	right	38.9	
M3CU	Toothrow Length C^s-M^3	left	39.1	
M3MU	Toothrow Length M^1-M^3	right	31.1	
M3MU	Toothrow Length M^1-M^3	left	31.5	
P4CU	Toothrow Length C^s-P^4	right	16.6	
P4CU	Toothrow Length C^s-P^4	left	16.8	
ALWU	Trans. Breadth Alv. Border At Mid. M^2		16.2	
PDEP	Depth Palate Midl. Bel. Horiz. Alv. Pl. at Mid. M^1		5.4	
AFAC	Angle Alv. Plane-Glpr Line		53.8º	
	// To Frankfurt Plane Or 30mm			
TMLN	Natm As % Nain		66.9	

*[aproxímate measurements]

Table 4
Mesopithecus pentelicus KRY: measurements of the mandible (in mm unless stated differently).

Mandible	KRY 5600
Thickness of corpus between M_1/M_2	9.5
Depth buccal at P_4	20.6
Depth buccal between M_1/M_2	19.1
Depth buccal middle M_3	21.3
Length C_i-M_3	42.7
Length C_i-P_4	18.3
Length M_1-M_3	24.3
Symphyseal angle	120º
$I = B/LM_1 \times 100$	81.3
$I = B/LM_2 \times 100$	84.7
$I = B/LM_3 \times 100$	74.3

Table 5
Measurements (in mm) of upper and lower dentition of the skull KRY5600 and isolated teeth.

	KRY 5600 upper dentition		KRY 2042	KRY 1000	KRY 7865	KRY 3462	KRY 5000		KRY5600 lower dentition	
	left	right	upper	upper	upper	upper	upper		left	right
L I^1	5.0	5.0						L I_1	3.2	3.3
B I^1	4.9	4.7	-	-	-	-	-	B I_1	4.3	4.3
L I^2	-	4.4	-	-	-	-	-	L I_2	3.3	3.3
B I^2	-	4.4	-	-	-	-	-	B I_2	4.5	4.6
L C^s	7.6	7.8	7.6	-	7.6	9.2	-	L C_i	4.8	4.9
B C^s	5.4	5.5	6.0	-	5.8	6.4	-	B C_i	7.0	7.1
L P^3	4.6	4.9	4.6	-	-	-	-	L P_3	6.4	6.2
B P^3	5.8	5.5	5.4	-	-	-	-	B P_3	4.2	4.2
L P^4	5.2	5.2	4.3	-	-	-	-	L P_4	6.2	5.6
B P^4	6.3	6.1	5.8	-	-	-	-	B P_4	4.5	4.6
L M^1	7.3	7.4	7.0	-	-	-	-	L M_1	7.2	7.2
Ba M^1	6.8	7.0	7.1	-	-	-	-	Ba M_1	5.5	5.4
Bp M^1	6.7	6.7	6.9	-	-	-	-	Bp M_1	5.8	5.6
L M^2	7.7	7.8	7.6	7.9	-	-	7.6	L M_2	7.7	7.8
Ba M^2	7.8	7.7	8.2	7.9	-	-	8.1	Ba M_2	6.3	6.3
Bp M^2	7.7	7.7	7.4	6.9	-	-	7.7	Bp M_2	6.5	6.5
L M^3	7.8	7.6	-	-	-	-	-	L M_3	9.6	9.6
Ba M^3	7.5	7.3	-	-	-	-	-	Ba M_3	6.9	6.5
Bp M^3	6.4	6.3	-	-	-	-	-	Bp M_3	6.5	6.3
L P^2-P^3	9.9	9.8	-	-	-	-	-	L P_2-P_3	11.8	11.7
L M^1-M^3	22.4	22.6	-	-	-	-	-	L M_1-M_3	24.3	24.2

L P^2-M^3	31.5	31.1	-	-	-	-	-	L P_2-M_3	36.1	35.8
L C^s-M^3	38.9	39.1	-	-	-	-	-	L C_i-M_3	42.6	42.4
L I^1-M^3	47.1	46.7	-	-	-	-	-	L I_1-M_3	48.3	48.2

L: Length; B: Breadth; a: anterior; p: posterior.

Table 6
Mesopithecus pentelicus KRY: measurements of the humerus (in mm) and indexes compared to those from Pikermi.

Variable number and acronym[a]	Measurement	KRY 5620	Pikermi females[a] (*n*=5)	Pikermi male(s)[a] (*n*=1-5)
1 (ART WID)	Width of distal articulation	19.3		
2 (MAX WID)	Distal maximum width	28.5		
3 (A/P WID)	Distal antero-posterior diameter	16.0		
4	Maximum height of the trochlea	15.9		
5 (OLE WID)	Width of the fossa olecrani	13.1		
6	Minimum height of the trochlea	8.8		
Index 1	Var. 1/Var. 2 × 100	68	62-73	59-69
Index 2	Var. 3/Var. 2 × 100	56	55-63	62
Index 3	Var. 4/Var. 1 × 100	82	66-90	83
Index 4	Var. 4/Var. 2 × 100	55	49-56	57
Index 5	Var. 4/Var. 3 × 100	99	77-100	91
Index 6	Var. 5/Var. 1 × 100	68	60-66	72
Index 7	Var. 5/Var. 2 × 100	46	40-45	49
Index 8	Var. 5/Var. 4 × 100	82	72-90	86

[a] Taken from or following Delson (1973)

Table 7

Mesopithecus pentelicus KRY: measurements of the ulna (in mm).

Ulna	Measurement	KRY 5621
1	Notch length	15.2
2	Width of proximal articular surface	12.5
3	Trochlea depth	6.1
4	Anteroposterior diameter of the proximal articular surface	18.0
5	Trochlea width	8.5
6	Maximum width of the proximal articular surface	15.2
7	Anteroposterior diameter at the beak	17.6
8	Width at 7	10.0
olec: DAP		13.0
olec: DT		10.7
Index 1	Var. 1/Var. 2 × 100	121.0

Table 8

Mesopithecus pentelicus KRY: measurements of the radius (in mm).

Radius	Measurement	KRY 1309
1	Distal width	18.3
2	Distal anteroposterior diameter	13.6
3	Width of the distal articular surface	15.9
4	Anteroposterior diameter of the distal articular surface	12.0

Table 9

Mesopithecus pentelicus KRY: measurements of the astragalus (in mm):

Astragalus	Measurement	KRY 8900	KRY 2773	KRY 2772
1	Length	24.7	21.2	21.1
2	Maximum width	18.2	14.4	14.7
3	Maximum trochlea length	15.5	12.8	12.1
4	Anterior trochlea width	12.8	10.9	10.5
5	Posterior trochlea width	9.8	8.5	8.0
6	Maximum anteroposterior diameter	16.5	12.5	13.3
7	Minimum trochlea anteroposterior diameter	11.1	9.2	9.4
8	Caput width	10.6	9.8	9.9
9	Caput anteroposterior diameter	11.4	8.5	9.4
10	Width of collum astragali	9.1	8.2	8.3
Index 1	Var. 2/Var. 1 × 100	74.0	68.0	69.7
Index 2	Var. 4/Var. 3 × 100	83.0	84.5	86.6
Index 3	Var. 5/Var. 4 × 100	76.5	78.3	76.4

Table 10
Mesopithecus pentelicus KRY: measurements of the calcaneus (in mm).

Calcaneus	Measurement	KRY 2770	KRY 2771
1	Maximum length	29.4	30.3
2	Length of manubrium	18.1	18.1
3	Maximum width	16.6	16.6
4	Anteroposterior diameter of tuber	12.9	12.4
5	Maximum diameter of the articular for cuboideum	9.7	-
6	Length of the articular surface for the astragalus	8.1	8.6
7	Width of sustentaculum tali	5.8	5.2
8	Maximum anteroposterior diameter	13.3	12.7
9	Tuber width	8.8	8.8
Index 1	Relative length of the manubrium (Var. 2/Var.1 × 100)	61.6	59.9
Index 2	Var. 3/Var.1 × 100	56.6	54.9

Table 11
Mesopithecus pentelicus KRY: measurements of the metapodials (in mm).

Metapodials	Measurement	KRY 7866	KRY 7868	KRY 7872	KRY 7873
1	Minimum width of the diaphysis	4.8	4.5	4.3	4.1
2	Anteroposterior diameter of the diaphysis	4.4	4.0	4.0	4.2
3	Distal width			6.2	6.1
4	Distal anteroposterior diameter			5.9	6.0

Table 12

Mesopithecus pentelicus KRY: measurements of the phalanges (in mm).

Phalanges	Measurement	KRY 7867	KRY 7869	KRY 7870	KRY 7871
1	Proximal width	7.9	7.5	6.9	6.5
2	Proximal dorsoplantar diameter	6.0	5.8	5.3	5.3

Table 13

Morphological characters of Kryopigi mandible of *Mesopithecus pentelicus* compared with various forms recognized in Greece according to Koufos (2008, 2009a, 2009b and references therein).

	Age (MN)	Localities	Size	Mandibular corpus	Strong symphyseal constriction	Anterior symphysis	Planum alverolare inclination	Fossa genioglossa	Inf. transv. torus	P_3 honimg facet	M_3 hypoconulid	Postcranials
Mesopithecus sp.	11	Nikiti-2 (NIK)										
M. delsoni	11	Ravin des Zouaves-5	Large	Deep	Yes	Flat	Slight	Large	Thick	Large	Well-developed bicuspid	
M. cf. *delsoni*	11-12	Ravin-X (R-X)	Similar to *M. delsoni* but not certainly ascribed to the species									
M. delsoni/pentelicus	12	Vathylakkos-2 Vathylakkos-3 Perivolaki	Large-medium	Relatively shallow	Yes	Flat	Slight back-wards	Large		Strong	Large with distal groove	Large
M. pentelicus	12	Pikermi Chomateri	Medium	Shallow H at P_4≈ H at M_3	No	Convex	Small - deeply inclined	Weak or absent		Small	Small	Intermediate
M. aff. *pentelicus*	13	Dytiko-2 (DIT) Dytiko-3 (DKO)	No mandible									
M. cf. *pentelicus*	13	Dytiko-1 (DTK)	Similar to *M. pentelicus*/not well-preserved material									
M. cf. *monspessulanus*	13	Dytiko-2 (DIT)	<*M. pentelicus*									
M. pentelicus	13/14	Maramena	*Mesopithecus* sp. according to Koufos (2009)									
M. pentelicus	12-13	Kryopigi (KRY)	Medium	Shallow (Fig. 3)	No	Convex	Small - deeply inclined	Barely visible	Slightly developed	Small	Small single cuspid	Intermediate

Table 14

Measurements (in mm) of the KRY5600 atlas compared to other colobines[a].

Measurements	KRY 5600	Asian colobines (n = 9)	*Colobus* sp. (n = 15)	*Procolobus verus* (n = 3)	*Piliocolobus* sp. (n = 5)
		Mean ± SD	Mean ± SD	Mean ± SD	Mean ± SD
Maximum dorso-ventral diameter	18.6	18.73 ± 5.50	19.38 ± 0.98	16.83 ± 0.89	18.83 ± 1.12
Canal: Dorso-ventral diameter	12.8	13.28 ± 3.86	13.61 ± 0.78	12.58 ± 0.94	13.28 ± 0.90
Anterior arc: cranio-caudal diameter	7.3	6.18 ± 1.79	6.57 ± 1.22	5.10 ± 1.20	6.18 ± 1.09
Anterior arc: dorso-ventral diameter	3.7	3.77 ± 1.17	3.81 ± 0.57	2.59 ± 0.51	3.84 ± 0.47
Height of the lateral mass (right side)	(11.0)	9.26 ± 2.95	9.66 ± 1.19	8.12 ± 1.04	8.69 ± 0.70
Maximum diameter upper articular facet	11.0	10.34 ± 2.96	11.13 ± 1.02	10.31 ± 0.68	10.03 ± 0.40
Minimum diameter (width) upper articular facet	6.5	4.73 ±1.36	4.81 ± 0.62	3.99 ± 0.29	3.89 ±0.26

Values in parentheses are estimated.

[a] For the exact sample composition see SOM Table S3.

SOM Table S1

Individuals and references used for Figure 6.

Specimen	Taxon	Sex	Reference
KRY5600	*M. pentelicus*	Male	This study
M305	*M. pentelicus*	Female	Delson, 1973
M424	*M. pentelicus*	Female	Delson, 1973
M311	*M. pentelicus*	Male	Delson, 1973
M316	*M. pentelicus*	Male	Delson, 1973
VTK-61	*M. pentelicus/delsoni*	Male	Koufos et al., 2004
K-333	*M. pentelicus*	Male	Koufos et al., 2003
K-335	*M. pentelicus*	Male	Koufos et al., 2003
HD-331	*M.* aff. *delsoni*	Male	Koufos et al., 2003
HD-462	*M.* aff. *delsoni*	Female	Koufos et al., 2003
London M8945	*M. pentelicus*	Male	Zapfe, 1991
LondonM8946	*M. pentelicus*	Male	Zapfe, 1991
LondonM8947	*M. pentelicus*	Male	Zapfe, 1991
LondonM8944	*M. pentelicus*	Male	Zapfe, 1991
ParisPik.014	*M. pentelicus*	Male	Zapfe, 1991
ParisPik.013	*M. pentelicus*	Male	Zapfe, 1991
ParisUniv.11	*M. pentelicus*	Male	Zapfe, 1991
ParisUniv.9	*M. pentelicus*	Male	Zapfe, 1991
BerlinMB1882/83.216.1	*M. pentelicus*	Male	Zapfe, 1991
Stuttgard	*M. pentelicus*	Male	Zapfe, 1991
Wien4693	*M. pentelicus*	Male	Zapfe, 1991
Wien4714	*M. pentelicus*	Male	Zapfe, 1991
ParisUniv.5	*M. pentelicus*	Female	Zapfe, 1991
BerlinMB1857-1	*M. pentelicus*	Female	Zapfe, 1991
MunchenASII7	*M. pentelicus*	Female	Zapfe, 1991
BaselPik.91	*M. pentelicus*	Female	Zapfe, 1991

SOM Table S2
Taxa and specimens used for GMM analysis in Figure 7.

AMNH = American Museum of Natural History (New York, USA), KNM = National Museums of Kenya (Nairobi, Kenya), KUPRI = Kyoto University Primate Research Institute (Inuyama, Japan), LGPUT = Laboratory of Geology and Paleontology, University of Thessaloniki (Thessaloniki, Greece), NHM = Natural History Museum (London, United Kingdom).

Taxon	Museum	Accession number
Allenopithecus nigroviridis	AMNH	52467
Lophocebus albigena	AMNH	52603
Cercocebus torquatus	AMNH	119757
Allenopithecus talapoin	AMNH	80779
Chlorocebus aethiops	KUPRI	CA14
Colobus guereza	AMNH	81070
Erythrocebus patas	AMNH	52576
Macaca sylvanus	AMNH	185277
Mandrillus sphinx	AMNH	119772
Mesopithecus pentelicus (Pikermi)	NHM	M.8947
Mesopithecus pentelicus (Kryopigi)	LGPUT	KRY5600
Nasalis larvatus	AMNH	103469
Papio hamadryas	KUPRI	4451
Presbytis melalophos	KUPRI	4512
Procolobus badius	AMNH	52283
Pygathrix nemaea	AMNH	87255
Rhinopithecus roxellana	AMNH	119648
Simias concolor	AMNH	103371
Theropithecus gelada	KUPRI	9030
Trachypithecus obscurus	AMNH	54970
Victoriapithecus macinnesi	KNM	MB 29100

SOM Table S3
Comparative atlas specimens used in this study.

Species	Institution		
	MNHN	RMCA	NHM
African colobines			
Piliocolobus badius	4F		
Piliocolobus foai		1F	
Procolobus verus	3 (2F, 1M)		
Colobus guereza	4	8 (4F, 2M, 2?)	
Colobus angolensis		3 (1F, 2M)	
Asian colobines			
Pygathrix nemaeus	1		
Semnopithecus entellus	1		
Nasalis larvatus	2 (2M)		2 (2M)
Trachypithecus phayrei	3 (1F, 1M, 1?)		

MNHN=Muséum national d'Histoire naturelle (Paris); RMCA=Royal Museum for Central Africa (Tervuren, Belgium); NHM=Natural History Museum (London).
M=male; F=female.

References

Delson, E., 1973. Fossil colobine monkeys of the circum-Mediterranean region and the evolutionary history of the Cercopithecidae (Primates, Mammalia). Ph.D. Dissertation, Columbia University.

Koufos, G.D., Spassov, N., Kovatchev, D., 2003. Study of *Mesopithecus* (Primates, Cercopithecidae) from the late Miocene of Bulgaria. Palaeontographica Abteilung A-Stuttgart 269, 39–91.

Koufos, G.D., Bonis, L. de, Kostopoulos, D., Viriot, L., Vlachou, T., 2004. *Mesopithecus* (Primates, Cercopithecoidea) from the Turolian locality of Vathylakkos 2 (Macedonia, Greece). Palaeontologische Zeitschrift 78, 213–228.

Zapfe, H., 1991. *Mesopithecus pentelicus* WAGNER aus dem Turolien von Pikermi bei Athen, Odontologie und Osteologie (Eine Documentation). Neue Denkschriften des Naturhistorisches Museum Wien 5, 12–203.